6) REMSAD Sulfur Simulation and Apportionment for BBNP

6.1 Introduction

The REMSAD air quality model was used to predict sulfate concentrations during the BRAVO study period (July–October 1999) and to estimate the sulfate contributions from regional sources that were impacting Big Bend NP during the study. REMSAD is used to estimate the chemical and physical processes that lead to the formation of sulfate particles, including emissions of sulfate precursors (namely sulfur dioxide), subsequent gas-phase and aqueous-phase oxidation of sulfur dioxide to particulate sulfate, transport of sulfate and its precursors via advection and turbulent diffusion, and wet and dry deposition, which constitute the principal loss mechanism for sulfate. REMSAD also simulates the occurrence of clouds, and their impact in rapidly transforming sulfur dioxide to particulate sulfate. An example of predicted sulfur dioxide and sulfate plumes from REMSAD is shown in Figure 6-1. The bulk of sulfur dioxide within the model domain is clearly dominated by sources in the eastern U.S. (Figure 6-1a), and individual point sources are evident in the western U.S. and Mexico. The Popocatepetl volcano, near Mexico City, is the dominant sulfur dioxide source in Mexico and is clearly evident in Figure 6-1a. The subsequent atmospheric oxidation of sulfur dioxide to sulfate particles results in the sulfate plume which is shown in Figure 6-1b. This sulfate plume is affected not only by the concentration of ambient sulfur dioxide but also by the presence of clouds, which are very effective at converting sulfur dioxide to sulfate via aqueous-phase reactions with hydrogen peroxide and ozone, and the presence of hydroxyl radical, which is the primary gas-phase oxidant of sulfur dioxide.

Input data to REMSAD include an emission inventory that defines the hourly emissions of chemical species such as sulfur dioxide, oxides of nitrogen, carbon monoxide, and various volatile organic compounds. Emission rates for these species are defined for each model grid cell. Meteorological data, including wind and temperature fields, precipitation rates, and cloud cover, are provided by the MM5 mesoscale weather model. Details about REMSAD's formulation and configuration for the BRAVO study can be found in section 2.2.1.

Four major sulfur dioxide source regions were considered for their contributions to predicted sulfate at Big Bend NP: 1) Texas, 2) Mexico, 3) the eastern U.S., and 4) the western U.S. (Figure 6-2). In addition to these four major source regions, the sulfate contributions from smaller subregions were also considered. These subregions include, for example, southeastern and northeastern Texas, the Ohio River Valley, and the Carbón I & II power plants located 250 km southeast of Big Bend NP. REMSAD was also used to investigate the impact of sulfur concentrations specified at the model boundary on simulated sulfate concentrations at Big Bend NP.

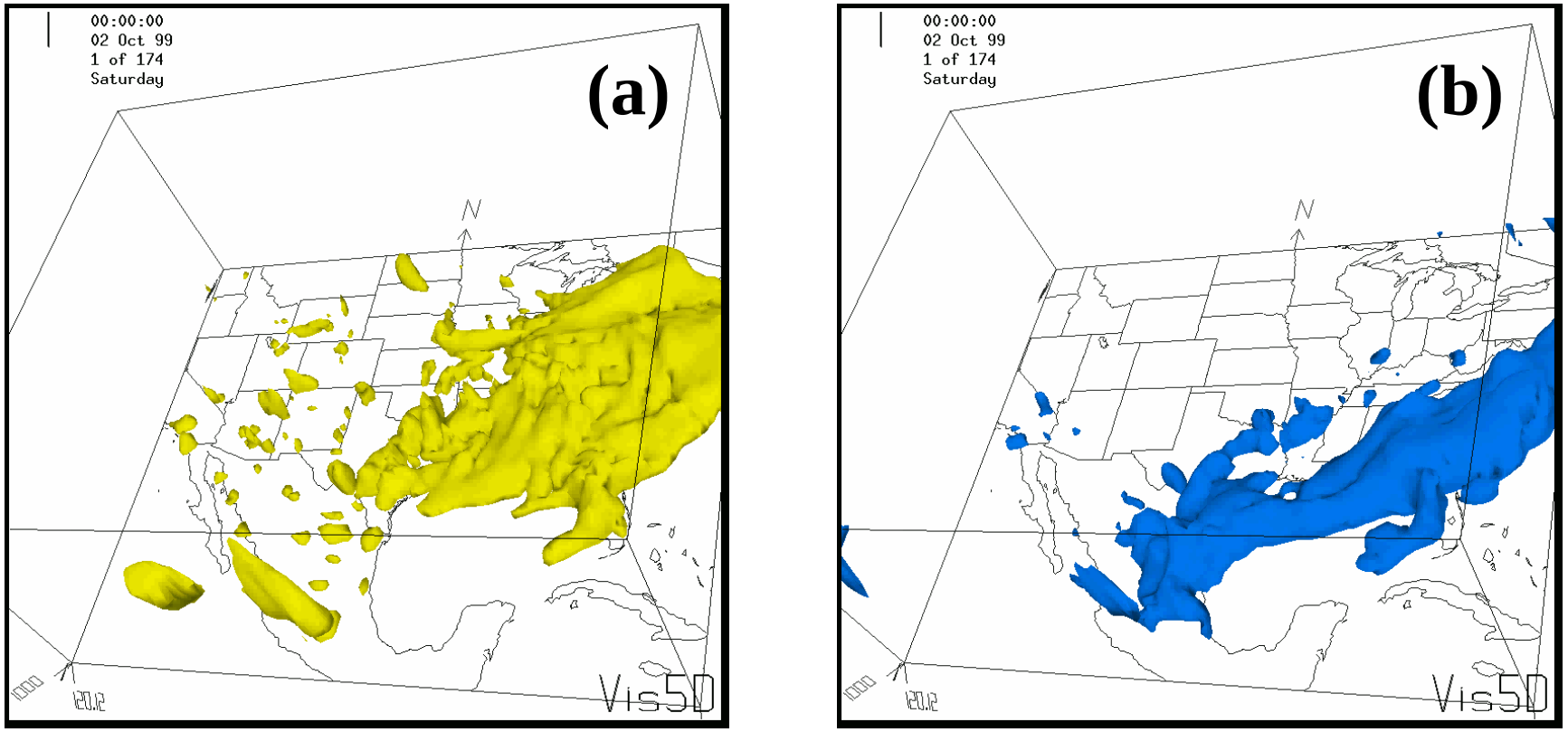

Figure 6-1. Plumes of (a) sulfur dioxide and (b) sulfate defined by 5 µg/m^3 isosurfaces for October 2, 1999.

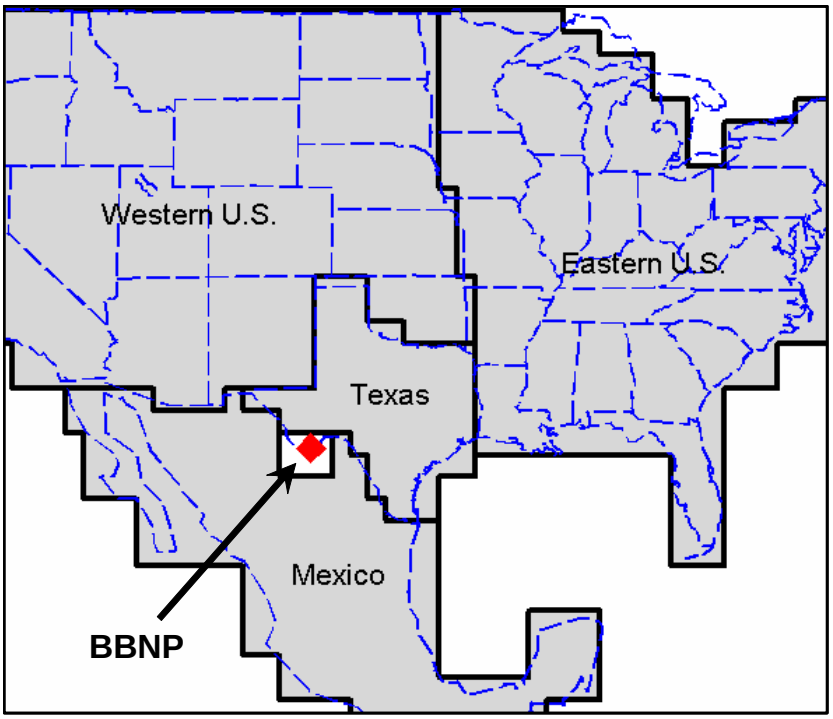

Figure 6-2. The four source regions evaluated for their impact on SO_4 predicted at BBNP: Mexico, Texas, the eastern U.S., and the western U.S.

Prior to applying REMSAD to the "emission sensitivity simulations" described above, the model's ability to predict "real world" sulfate concentrations during the four month BRAVO period was assessed. Therefore a "base simulation" was developed and statistically evaluated to determine the model's skill at predicting sulfate concentrations at Big Bend NP and at other monitoring sites located throughout the model domain. This base simulation specified sulfur dioxide emissions from coal-fired power plants, smelters, petroleum refineries, and other sources at their normal emission rates. Sulfate concentrations predicted by this REMSAD base simulation were compared to the observed concentrations collected at the sulfate monitors deployed throughout Texas during the BRAVO study, as well as the larger network of CASTNET monitors that are located throughout the U.S. This combination of 37 BRAVO monitoring sites and 67 CASTNET monitoring sites (that fall within the REMSAD model domain) provides the large-scale spatial coverage that is necessary to adequately assess model performance and to identify regions of the modeling domain where biases might exist. It is also of interest to examine the statistical evaluation over different time periods, e.g., daily versus monthly, as this can elucidate trends that exist on synoptic or seasonal time scales.

After the REMSAD base simulation has been established, the emissions sensitivity simulations can be performed to determine the impact of emissions from regional and subregional sulfur dioxide sources on predicted sulfate at Big Bend NP. The emission sensitivity simulations are run by repeating the original base simulation, with the one difference being that all sulfur dioxide emissions from the source region of interest are removed. Primary particulate sulfate emissions, which constitute less than a few percent of the total sulfur emissions, are also removed. The impact of sulfur dioxide emissions from a source region on sulfate predicted at a downwind receptor is defined as the difference between the sulfate concentration predicted by the original base simulation and the sulfate concentration from the emission sensitivity

simulation. Several factors can influence whether emissions from a source region will have an appreciable impact on a receptor site (e.g., Big Bend NP), including whether the receptor is frequently downwind of the source region, the magnitude of the emissions from the source region, and the percentage of sulfur dioxide that is oxidized to sulfate en route to the receptor.

An interesting aspect of this work was an investigation of REMSAD's response to two types of emission sensitivity simulations. The sulfate attribution results presented in this chapter were derived from the emission sensitivity simulations described above, where REMSAD was run after sulfur dioxide emissions from a source region were removed. These simulations are termed "emissions out" simulations. There is, however, a complementary approach where sulfur dioxide emissions from a source region can be retained, but sulfur dioxide emissions outside of the source region are removed. These simulations are termed "emissions in" simulations. An important question is whether the sulfate attributions derived from the "emissions out" simulations are equivalent to the "emissions in" simulations. The attributions between the two methods will be equivalent if sulfate concentrations predicted by REMSAD respond in direct proportion to changes in sulfur dioxide emissions. Results from this study show that these two approaches to performing emissions sensitivity simulations, i.e., "emissions out" and "emissions in", are indeed very nearly equivalent, and hence only results from the "emissions out" simulations will be presented. Further details on this topic can be found in section 6.3.

The following sections of this chapter are divided into three major topics: a statistical evaluation of REMSAD's skill in predicting sulfate concentrations during the four month BRAVO study (section 6.2), an investigation of the degree of linearity in REMSAD's sulfate predictions with regard to the "emissions out" and "emissions in" simulations (section 6.3), and the results of the emission sensitivity simulations to determine the attributions from regional and subregional emission sources to sulfate predicted at Big Bend NP (section 6.4).

6.2 Evaluation of REMSAD Base Simulation

As described above, the REMSAD regional air quality model was used to create a base simulation for the July–October 1999 BRAVO period. This base simulation used an emission inventory that was estimated at "real world" levels and was designed to evaluate the model's skill in predicting the formation and transport of particulate sulfate during the BRAVO field study. An example of surface-level sulfate predicted by REMSAD is shown in Figure 6-3, where concentrations range from < 1 $\mu g/m^3$ in remote and maritime areas to well over 15 $\mu g/m^3$ in regions downwind of large sulfur dioxide sources. The patterns evident in Figure 6-3 are a result of several factors, including the emissions of sulfur dioxide in the atmosphere, the presence of clouds which rapidly convert sulfur dioxide to sulfate, wind patterns, and rates of deposition. An interesting aspect of Figure 6-3 is the strong concentration gradients that exist in proximity to Big Bend NP; their potential impact with regard to model evaluation will be considered in the following sections.

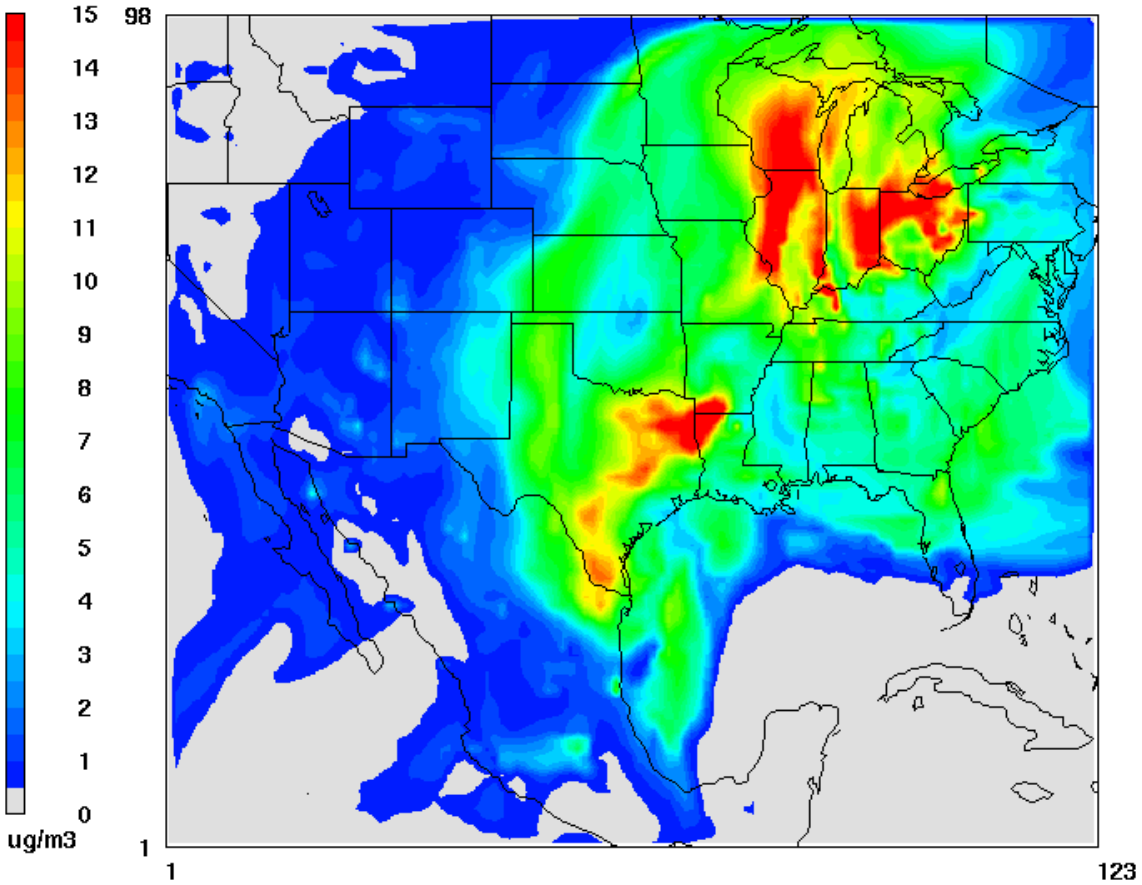

Figure 6-3. Ground-level sulfate concentrations (µg/m^3) predicted by the REMSAD air quality model for 1500 CST, September 1, 1999.

An evaluation of REMSAD's predictive skill was conducted by comparing simulated sulfate concentrations with observed concentrations. Sulfate observations were collected from either the BRAVO or CASTNET monitoring networks. The BRAVO monitoring network measured daily-average sulfate concentrations and consisted of 37 sites that were deployed throughout Texas during the four months of the study. The CASTNET monitoring network has a much broader coverage, with monitoring sites concentrated in the northeastern portion of the U.S. The CASTNET monitoring network collects samples on a weekly average, and 67 of these monitors lie within the REMSAD model domain. The BRAVO and CASTNET monitoring sites are shown in Figures 6-4 and 6-5, respectively.

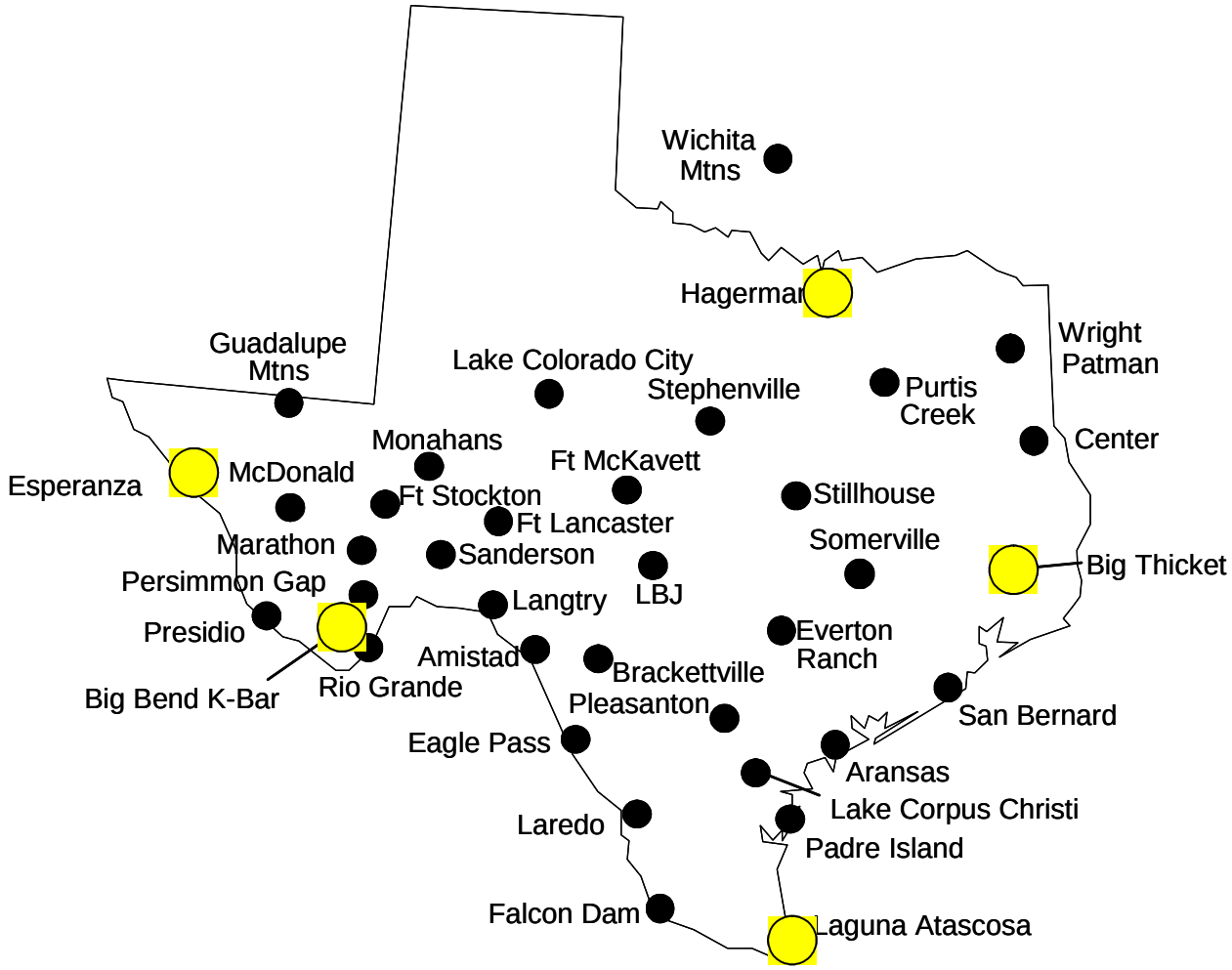

Figure 6-4. The BRAVO monitoring network. Example time series plots and statistics are presented for highlighted monitors.

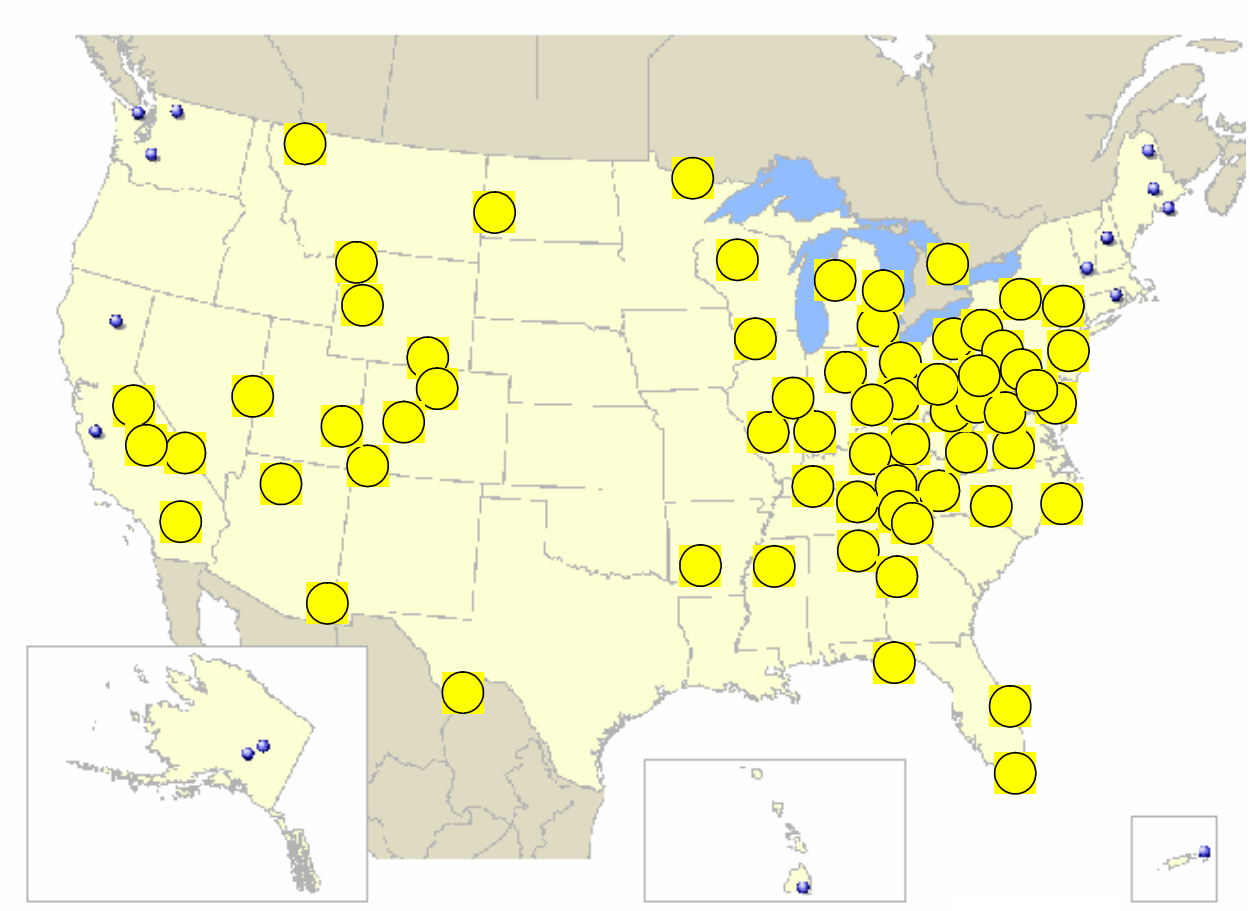

Figure 6-5. The CASTNET monitoring network. Highlighted monitors fall within the REMSAD model domain.

The performance evaluation of the base simulation will be presented in four major components:

1) Time series plots and statistics of predicted versus observed sulfate at Big Bend NP and at four sites that lie north, east, south, and west of Big Bend NP.
2) Scatter plots and statistics of predicted versus observed sulfate for all 37 BRAVO monitors.
3) Scatter plots and statistics of predicted versus observed sulfate for the 67 CASTNET monitors that fall within the model domain.
4) Contour maps showing spatial patterns of model bias and error.

Statistics used to assess model performance include the correlation coefficient (R), normalized bias (Bn), and normalized error (En). The normalized bias is defined as

$$Bn = \frac{1}{N}\sum_i \left(\frac{P_i - O_i}{O_i} \right) \qquad (6\text{-}1)$$

and the normalized error is defined as

$$En = \frac{1}{N}\sum_i \left| \frac{P_i - O_i}{O_i} \right| \quad (6\text{-}2)$$

It should be noted that both Bn and En are susceptible to over-weighting over-predictions as compared to under-predictions (for the normalized difference shown above the under-predictions are bounded by -1 while over-predictions can grow arbitrarily large). To help minimize skewing of Bn and En, observations less than 0.1 $\mu g/m^3$ are not included in the statistical analysis. Observations less than this 0.1 $\mu g/m^3$ threshold represent a very small portion of the measured sulfate values. All observations and predictions are paired in space and time, i.e., there is no temporal or spatial averaging (except for the case of the contour maps of Bn and En in section 6.2.4, where the daily BRAVO network data was converted to a weekly average to match the CASTNET network data). It should be noted that the statistics calculated for the four month average may not necessarily match the average of the monthly statistics, as several of the months contain missing data.

All four of the assessments listed above will be presented on a monthly basis (July, August, September, and October 1999) and on an overall study basis (the four month average of July–October 1999). The purpose of examining model performance on a monthly basis will be to elucidate seasonal trends in the model predictions. Performance on a daily time scale will be apparent through the time series plots presented for the Big Bend NP monitor and the four peripheral monitors of the BRAVO network. Finally, spatial patterns derived by combining both the BRAVO and CASTNET networks will indicate which regions within the model domain are most likely to experience bias.

6.2.1. BRAVO Network: Big Bend NP and Four Peripheral Monitors

Time series plots of the daily predicted and observed sulfate at Big Bend NP and four peripheral sites within the BRAVO monitoring network are shown in Figure 6-6, and model performance statistics are shown in Table 6-1. At the K-Bar monitor in Big Bend NP (Figure 6-6a), observed sulfate concentrations range from < 1 $\mu g/m^3$ to over 9 $\mu g/m^3$, with the periods of peak sulfate levels occurring between mid-August and October. This period corresponds to a transition of wind flow patterns, where transport primarily from Mexico in July and early August yields to transport from eastern Texas and the eastern U.S. during mid-August through October. Although REMSAD frequently predicts the correct timing of sulfate peaks, there is a clear bias to underestimate sulfate concentrations during the first half of the study, with a normalized bias of predicted sulfate of -41% and -43% for July and August, respectively. This negative bias may indicate that Mexican sulfur dioxide emissions are underestimated, as flow from Mexico dominates during this period, or that sulfur dioxide from Mexican sources is not being oxidized rapidly enough en route to Big Bend NP. From the latter half of August until the end of October, sulfate concentrations are higher, with a peak observed sulfate concentration of 9 $\mu g/m^3$ recorded on September 1 at the K-Bar monitor. Again, the timing of the predicted peak concentrations generally appears to be in good agreement with the observations. There are, however, a few notable exceptions, such as the 5 $\mu g/m^3$ peak that was observed September 27–29. This episode is clearly not evident in the predicted time series at any of the three monitors, although concentrations of this magnitude were predicted within 100 km of Big Bend NP, as shown in Figure 6-7. Also, there appears to be a shift in the timing of the mid-October sulfate peak, with the predicted maximum occurring October 9 while the actual maximum was observed October

12. The four-month observed and predicted sulfate concentrations at Big Bend NP were 2.0 $\mu g/m^3$ and 2.5 $\mu g/m^3$, respectively.

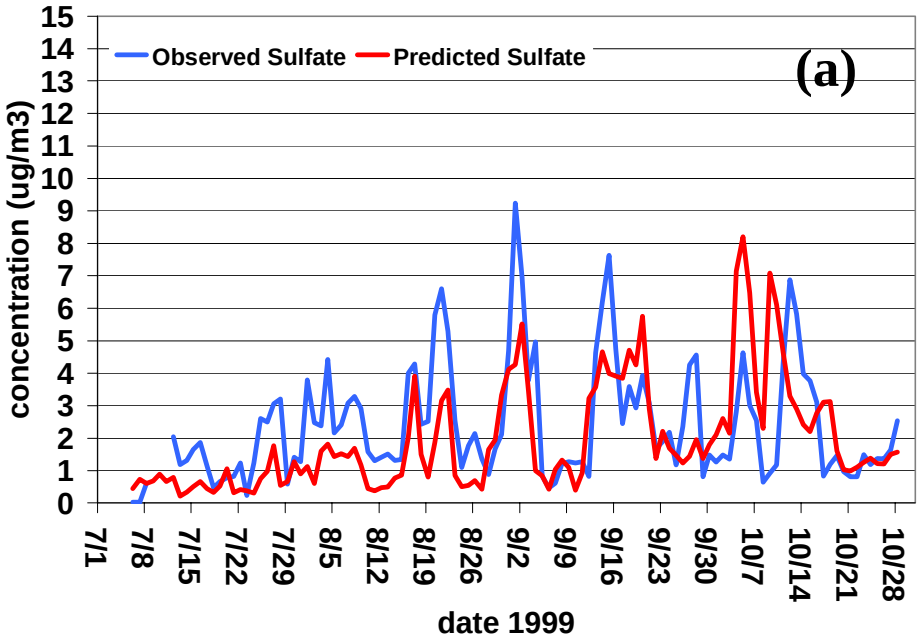

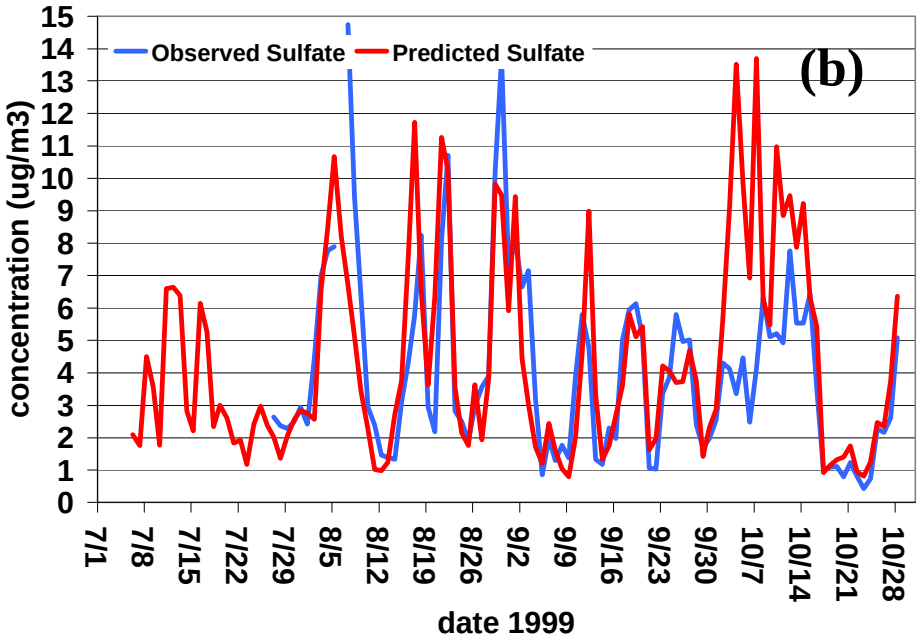

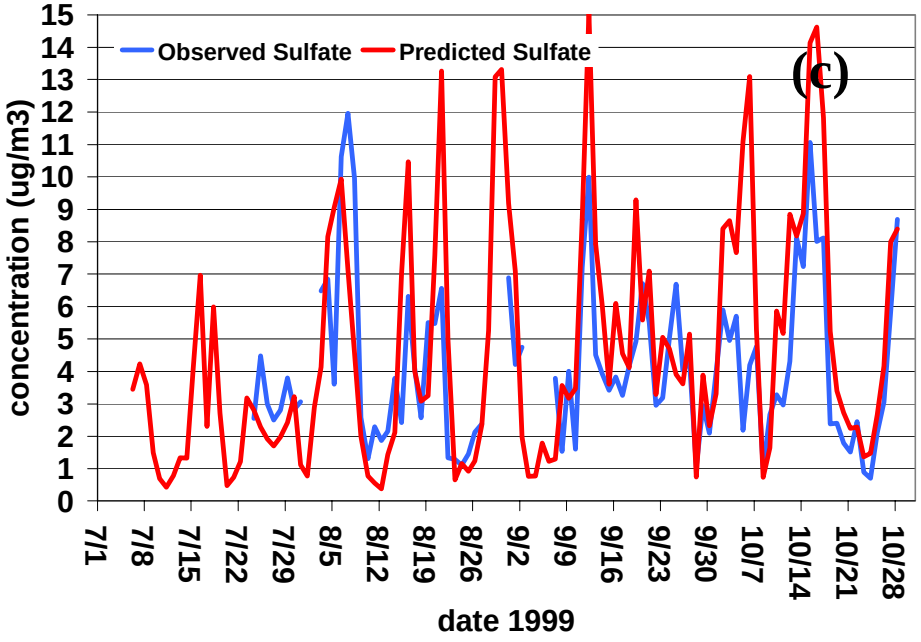
Observed Sulfate
Predicted Sulfate
(c)
concentration (ug/m3)
0
1
2
3
4
5
6
7
8
9
10
11
12
13
14
15
7/1
7/8
7/15
7/22
7/29
8/5
8/12
8/19
8/26
9/2
9/9
9/16
9/23
9/30
10/7
10/14
10/21
10/28
date 1999

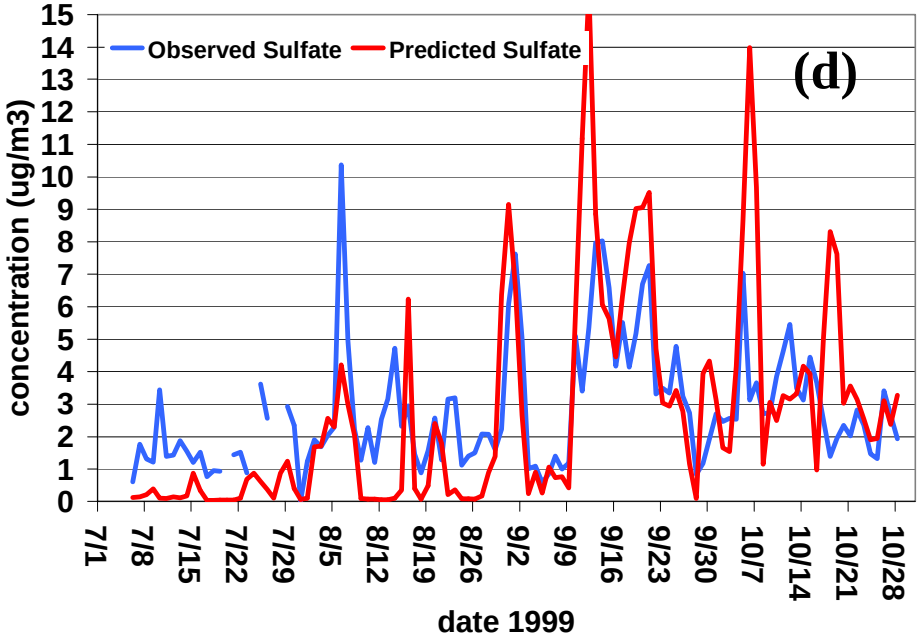
Observed Sulfate
Predicted Sulfate
(d)
concentration (ug/m3)
0
1
2
3
4
5
6
7
8
9
10
11
12
13
14
15
7/1
7/8
7/15
7/22
7/29
8/5
8/12
8/19
8/26
9/2
9/9
9/16
9/23
9/30
10/7
10/14
10/21
10/28
date 1999

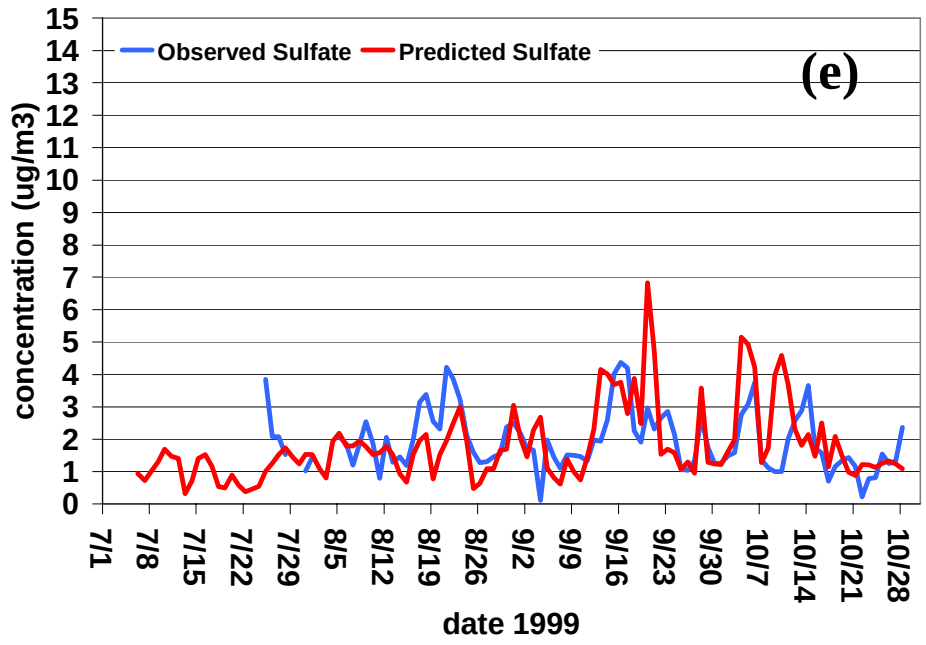

Figure 6-6. Observed and predicted sulfate time series for five monitors within the BRAVO network: (a) K-Bar, (b) Hagerman, (c) Big Thicket, (d) Laguna Atascosa, and (e) Esperanza.

Table 6-1. REMSAD performance statistics for the base simulation calculated at Big Bend NP (K-Bar) and four peripheral sites (Hagerman – northern Texas, Big Thicket – eastern Texas, Laguna Atascosa – southern Texas, Esperanza – western Texas).

	Overall	July 99	August 99	September 99	October 99
K-Bar					
Observed Average (µg/m^3)	2.5	1.3	2.7	3.1	2.3
Predicted Average (µg/m^3)	2.0	0.6	1.5	2.5	3.0
R	0.50	0.46	0.69	0.67	0.32
Normalized Error	62%	51%	53%	43%	98%
Normalized Bias	1%	-41%	-43%	2%	78%
Data Completeness	98%	88%	100%	100%	100%
Hagerman					
Observed Average (µg/m^3)	4.1	2.1	5.5	3.6	3.4
Predicted Average (µg/m^3)	4.6	2.2	5.3	3.4	5.6
R	0.66	0.21	0.71	0.75	0.73
Normalized Error	44%	16%	38%	36%	64%
Normalized Bias	23%	-15%	6%	7%	64%
Data Completeness	84%	23%	97%	100%	100%
Big Thicket					
Observed Average (µg/m^3)	4.2	2.8	4.3	4.2	4.3
Predicted Average (µg/m^3)	5.1	2.3	4.6	5.0	6.4

R	0.70	-0.47	0.65	0.75	0.78
Normalized Error	54%	34%	58%	43%	66%
Normalized Bias	27%	-28%	11%	24%	59%
Data Completeness	79%	35%	84%	87%	100%
Laguna Atascosa					
Observed Average (µg/m^3)	2.9	1.6	2.6	3.8	3.0
Predicted Average (µg/m^3)	2.9	0.3	1.6	4.7	4.1
R	0.60	0.39	0.50	0.70	0.19
Normalized Error	70%	81%	70%	58%	77%
Normalized Bias	-7%	-81%	-43%	18%	52%
Data Completeness	96%	85%	100%	100%	100%
Esperanza					
Observed Average (µg/m^3)	2.0	1.8	2.1	2.0	1.7
Predicted Average (µg/m^3)	2.0	1.3	1.6	2.3	2.1
R	0.43	-0.09	0.58	0.54	0.48
Normalized Error	71%	41%	31%	112%	72%
Normalized Bias	38%	-15%	-15%	81%	54%
Data Completeness	82%	23%	90%	100%	100%

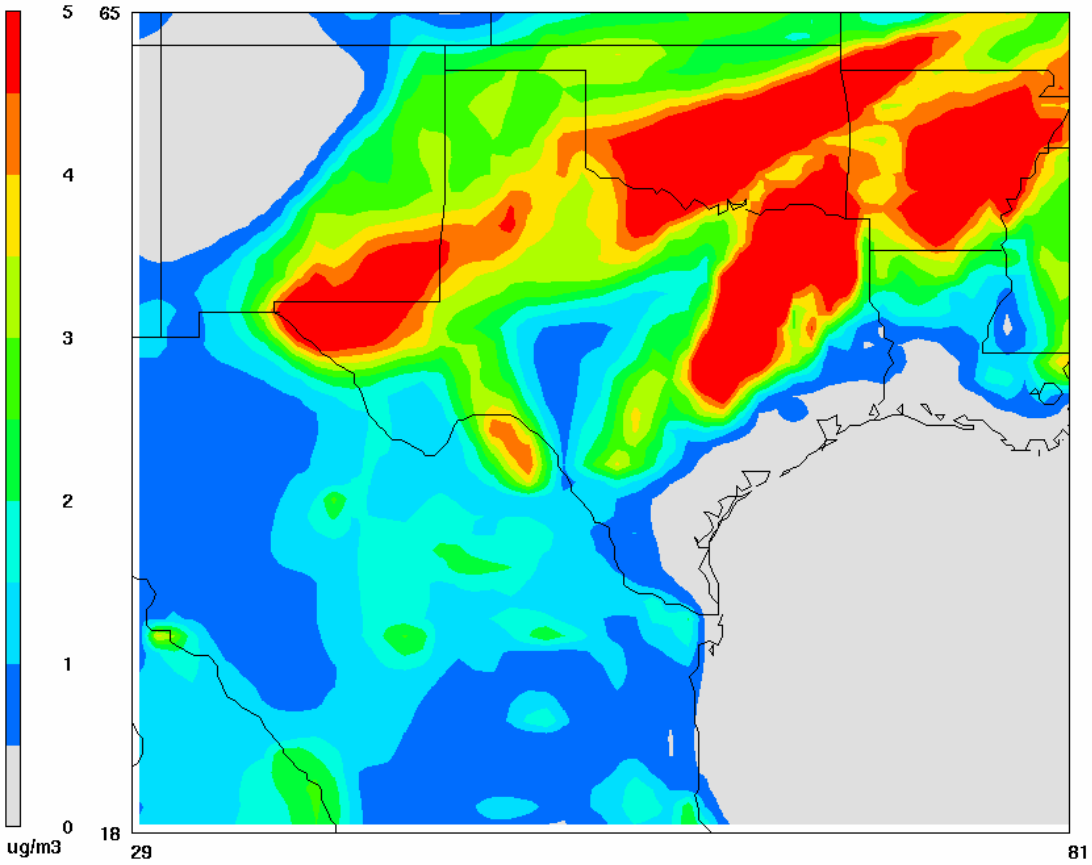

Figure 6-7. Ground-level sulfate concentrations (µg/m^3), September 28, 1999.

Figures 6-6b to 6-6e show time series plots of four sites that represent the periphery of the BRAVO monitoring network. These include the Hagerman monitor in northern Texas, the Big Thicket monitor in eastern Texas, the Laguna Atascosa monitor in southern Texas, and the Esperanza monitor in western Texas. In general, the northern and eastern monitors of Hagerman (Figure 6-6b) and Big Thicket (Figure 6-6c), respectively, show higher sulfate concentrations. Four month average observed and predicted sulfate concentrations at Hagerman are 4.1 $\mu g/m^3$ and 4.6 $\mu g/m^3$, respectively, and 4.2 $\mu g/m^3$ and 5.1 $\mu g/m^3$, respectively, at Big Thicket. Sulfate concentrations are lower at the southern monitor of Laguna Atascosa, with average observed and predicted sulfate concentrations of 2.9 $\mu g/m^3$, and lower still at the western monitor of Esperanza, with average observed and predicted sulfate concentrations of 2.0 $\mu g/m^3$. From Table 6-1 it is apparent for all five monitoring sites that REMSAD has a tendency to under-predict sulfate concentrations during July with normalized biases ranging between -15% and -81%, and over-predict sulfate concentrations during October, with normalized biases ranging between 52% and 78%.

6.2.2. BRAVO Network: Aggregation of 37 BRAVO Monitors

To assess REMSAD's performance over the entire BRAVO monitoring network, the observed and predicted sulfate concentrations were aggregated and evaluated on an overall and monthly basis (Figure 6-8 and Table 6-2). The four month observed and predicted sulfate concentrations were 3.1 $\mu g/m^3$ and 3.3 $\mu g/m^3$, respectively. Other performance measures for this period were R = 0.61, Bn= 19%, and En = 65%. There was a significant under-prediction of sulfate in July (Figure 6-8b), and a significant over-prediction in October (Figure 6-8e); corresponding biases for these two months were -38% and 82%, respectively. Model performance is best during the months of August (R = 0.75, Bn = -25%, En = 49%) and September (R = 0.63, Bn = 30%, En = 61%).

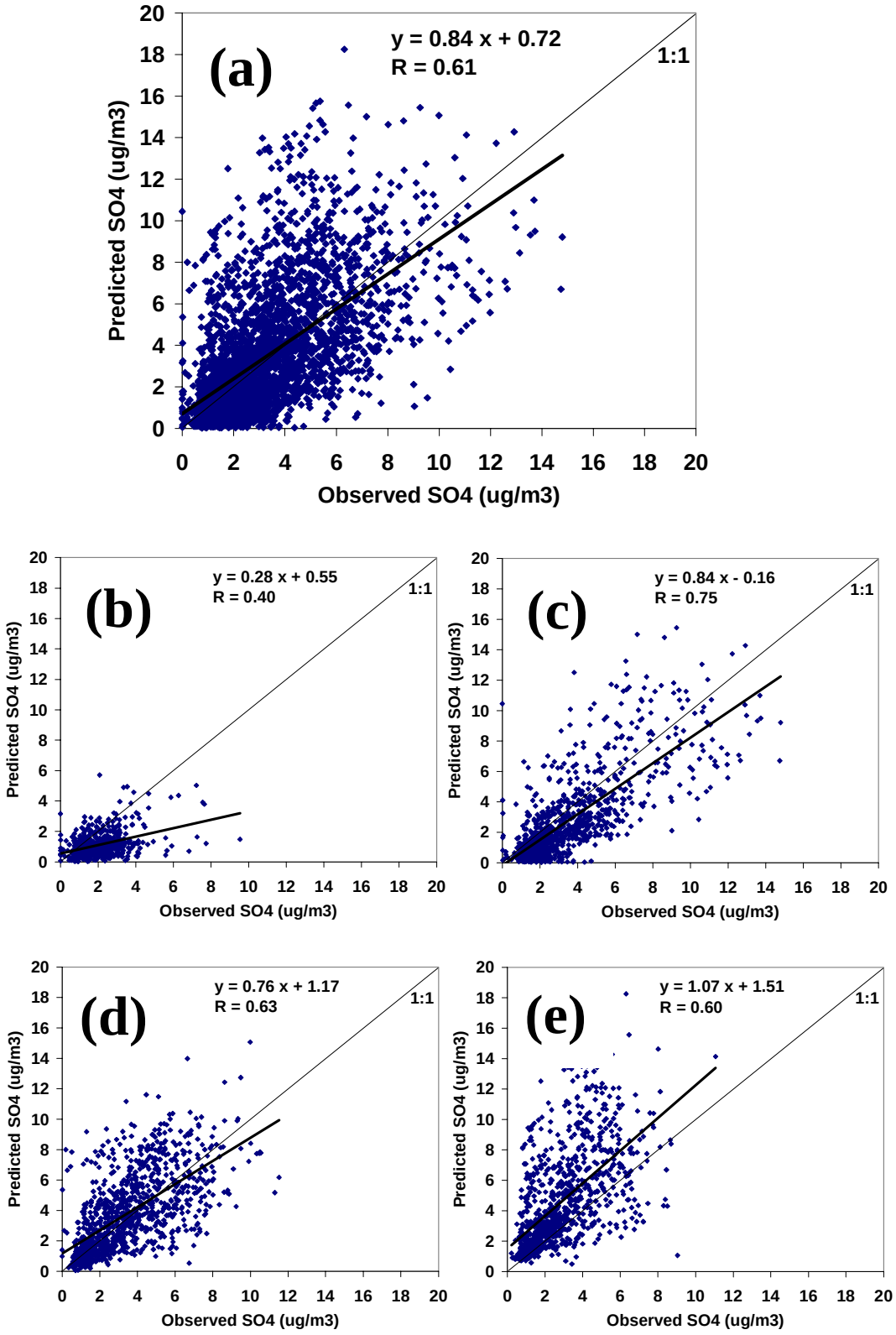

Figure 6-8. Scatter plots of predicted versus observed sulfate concentrations for all 37 BRAVO monitors: (a) July–October, (b) July, (c) August, (d) September, and (e) October. A least-squares linear regression equation and line is also shown.

Table 6-2. REMSAD performance statistics for the base simulation calculated for all 37 BRAVO monitors.

	Overall	July 99	August 99	September 99	October 99
Observed Average (μg/m^3)	3.1	2.1	3.5	3.5	2.8
Predicted Average (μg/m^3)	3.3	1.1	2.8	3.8	4.6
R	0.61	0.40	0.75	0.63	0.60
Normalized Error	62%	51%	53%	43%	98%
Normalized Bias	1%	-41%	-43%	2%	78%
Data Completeness	98%	88%	100%	100%	100%

6.2.3. CASTNET Network: Aggregation of 67 CASTNET Monitors

To investigate REMSAD's performance over a larger scale, the observed and predicted sulfate from the 67 CASTNET monitors that lie within the model domain were aggregated and evaluated on an overall and monthly basis (Figure 6-9 and Table 6-3). Unlike the BRAVO monitoring network, the CASTNET observations are collected weekly instead of daily, and hence the REMSAD predictions were averaged over the same weekly interval as the CASTNET observations. Observed and predicted sulfate concentrations from the CASTNET sites were significantly higher as compared to the BRAVO network due to the large number of CASTNET monitors located within the northeastern U.S. Overall observed and predicted sulfate concentrations were 4.5 μg/m^3 and 5.0 μg/m^3, respectively. REMSAD model performance was significantly better when evaluated against the CASTNET observations as compared to BRAVO observations; this is due at least in part to the longer temporal average of the CASTNET data. Overall performance statistics were R = 0.90, Bn = 21%, and En = 45%. Model performance on a monthly basis was best during the first three months of the study period, with R ranging between 0.88 and 0.92, Bn ranging between 3% and 21%, and En ranging between 36% and 43%. Similar to the previous discussion, significant over-predictions are evident in October, with Bn = 50% and En = 65%.

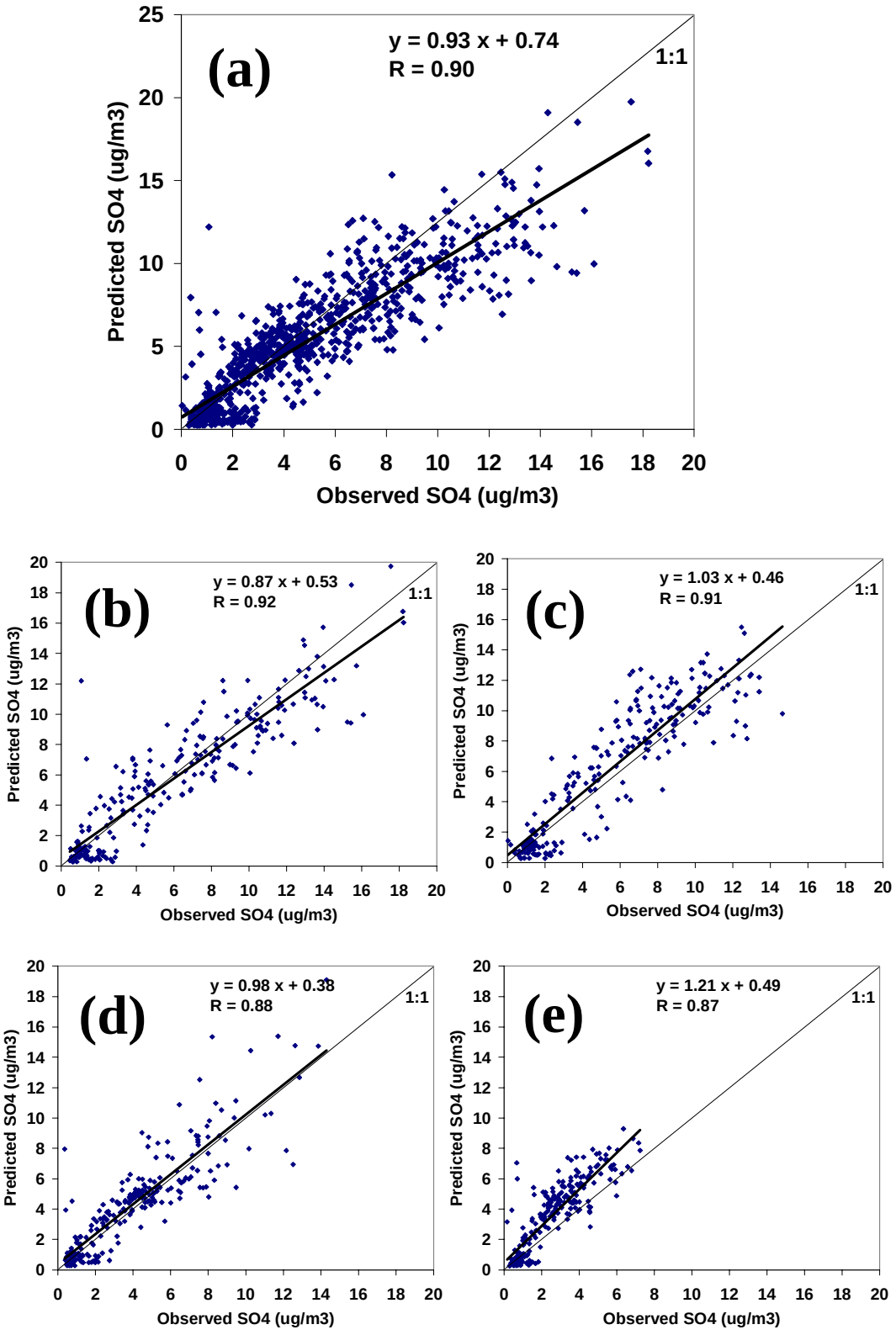

Figure 6-9. Scatter plots of predicted versus observed sulfate concentrations for the 67 CASTNET monitors that lie within the REMSAD model domain: (a) July–October, (b) July, (c) August, (d) September, and (e) October. A least squares linear regression equation and line is also shown.

Table 6-3. REMSAD performance statistics for the base simulation calculated for the 67 CASTNET monitors that fall within the model domain.

	Overall	July 99	August 99	September 99	October 99
Observed Average (µg/m^3)	4.5	5.8	5.6	4.1	2.6
Predicted Average (µg/m^3)	5.0	5.6	6.2	4.5	3.6
R	0.90	0.92	0.91	0.88	0.87
Normalized Error	45%	36%	36%	43%	65%
Normalized Bias	21%	3%	12%	21%	50%
Data Completeness	97%	99%	97%	96%	97%

6.2.4. Spatial Patterns of Model Bias

A final aspect of the model evaluation of the base simulation was to examine how model performance varied spatially across the domain. Contour maps of normalized bias are shown in Figure 6-10. These maps were created by aggregating all of the available sulfate data from the BRAVO and CASTNET monitoring networks, and calculating weekly averages for the BRAVO sulfate concentrations to match the time scale of the CASTNET concentrations. The overall four month average bias is shown in Figure 6-10a. In general, Bn ranges between -25% and 25% for BRAVO monitors in Texas and rises towards the northeast, where Bn can exceed 50%. On a monthly basis, the lowest biases are evident in July. It is particularly interesting to note the gradient of Bn that exists for the Texas monitors during this month, with Bn ranging between -45% and -84% at sites near the Texas/Mexico border. This gradient is also apparent to a lesser extent in August. September and October see a transition towards positive values of Bn, especially in Texas and the Midwest (Figures 6-10d and 6-10e, respectively).

(a)

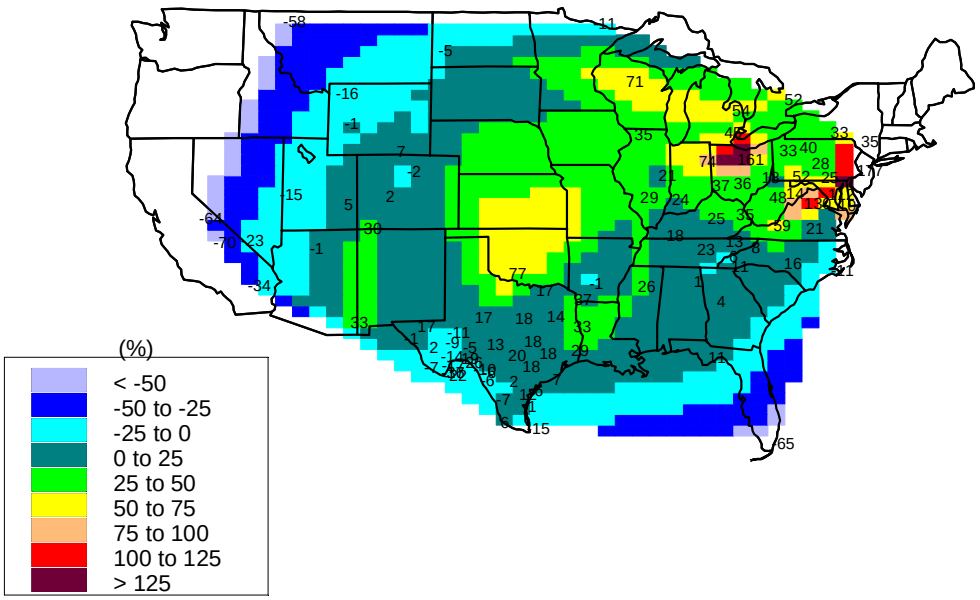

(b)

SO4 Normalized Bias (%)
July 1999

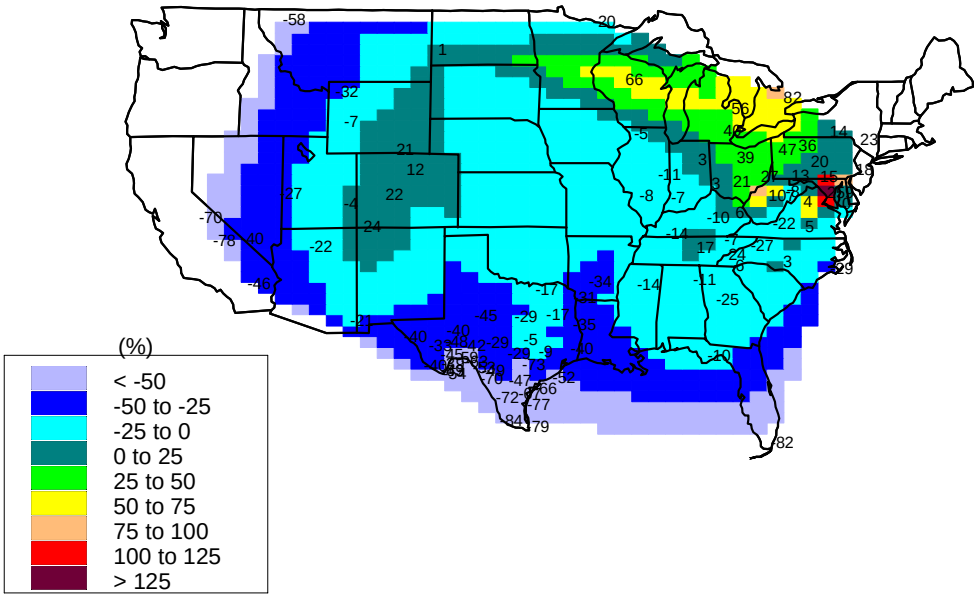

(c)

SO4 Normalized Bias (%)
Aug 1999

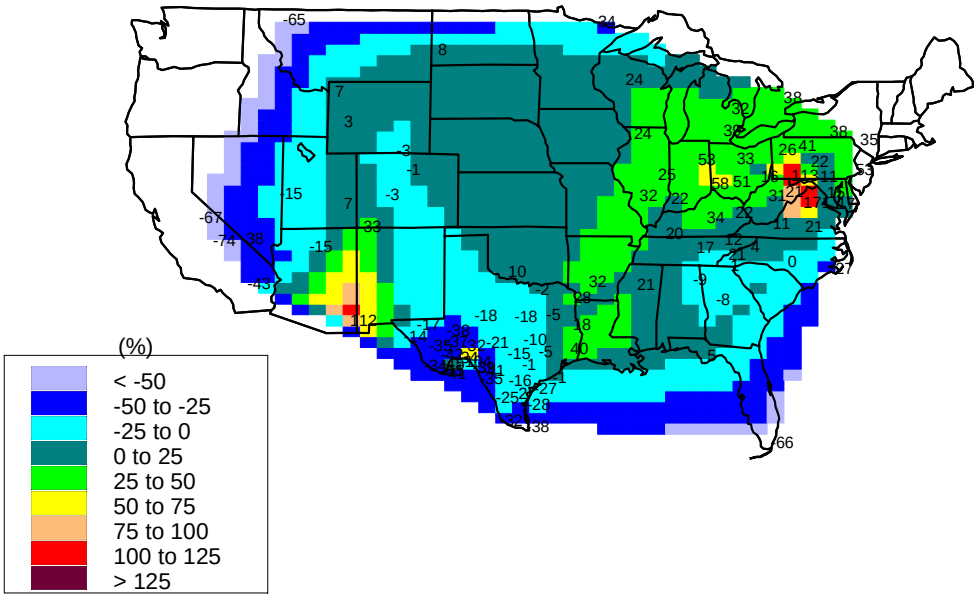

(d)

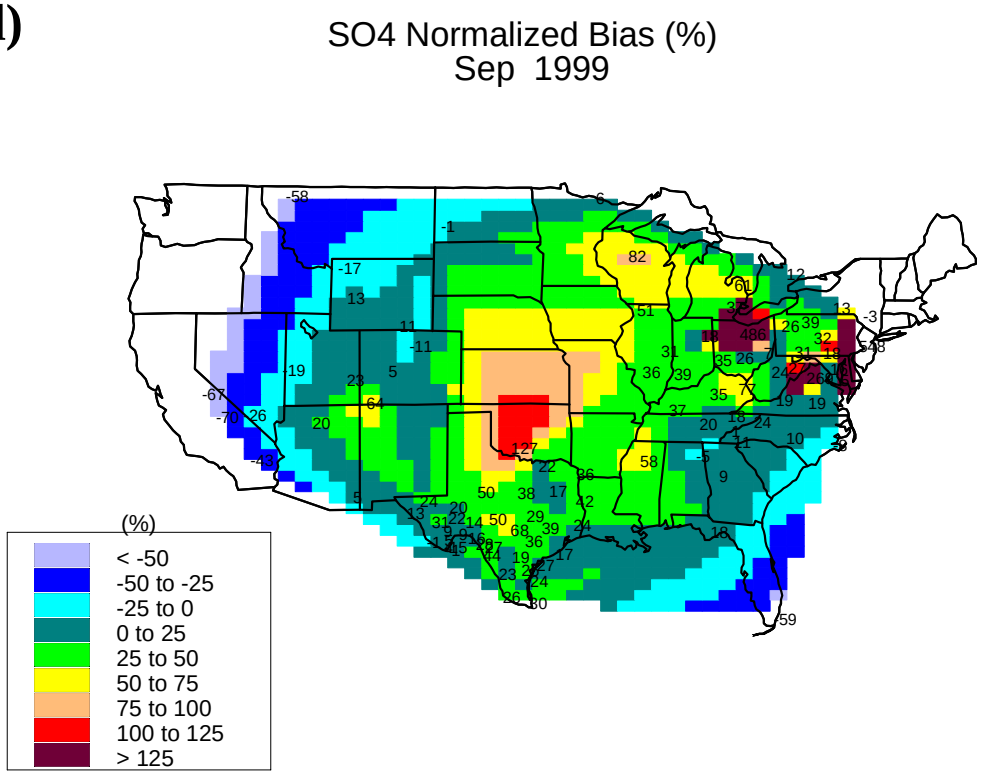

(e)

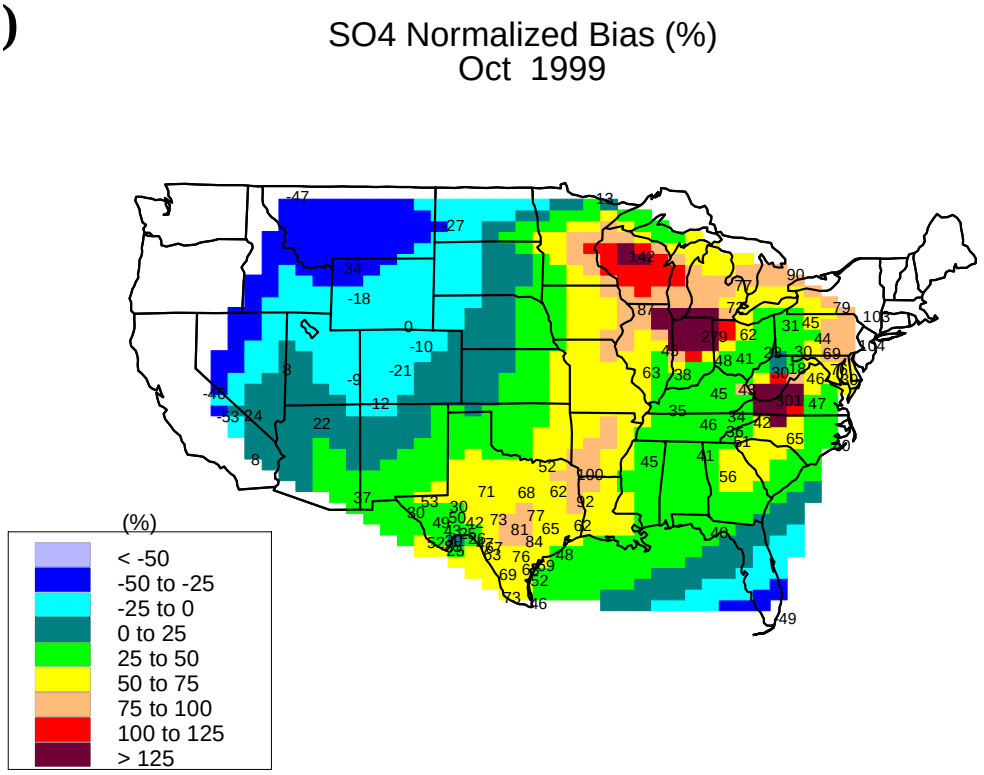

Figure 6-10. Contour maps of interpolated normalized bias: (a) July–October, (b) July, (c) August, (d) September, and (e) October.

6.3 Linearity of Sulfate Predictions

As discussed earlier, the emissions sensitivity simulations were conducted by removing sulfur dioxide (and primary sulfate) emissions from a source region, and comparing the resulting sulfate prediction to the original base simulation. These simulations, where sulfur dioxide was removed from the source region of interest, were termed "emissions out" sensitivity simulations. A complementary set of "emissions in" simulations was also evaluated where sulfur emissions were retained for the source region of interest but removed elsewhere. Examples of the emission inventory modifications that were performed for these two sets of simulations are shown in Figure 6-11. It should be noted that only sulfur dioxide and primary sulfate emissions were modified, and emissions of volatile organic compounds, oxides of nitrogen, carbon monoxide, etc., were left at their base case levels.

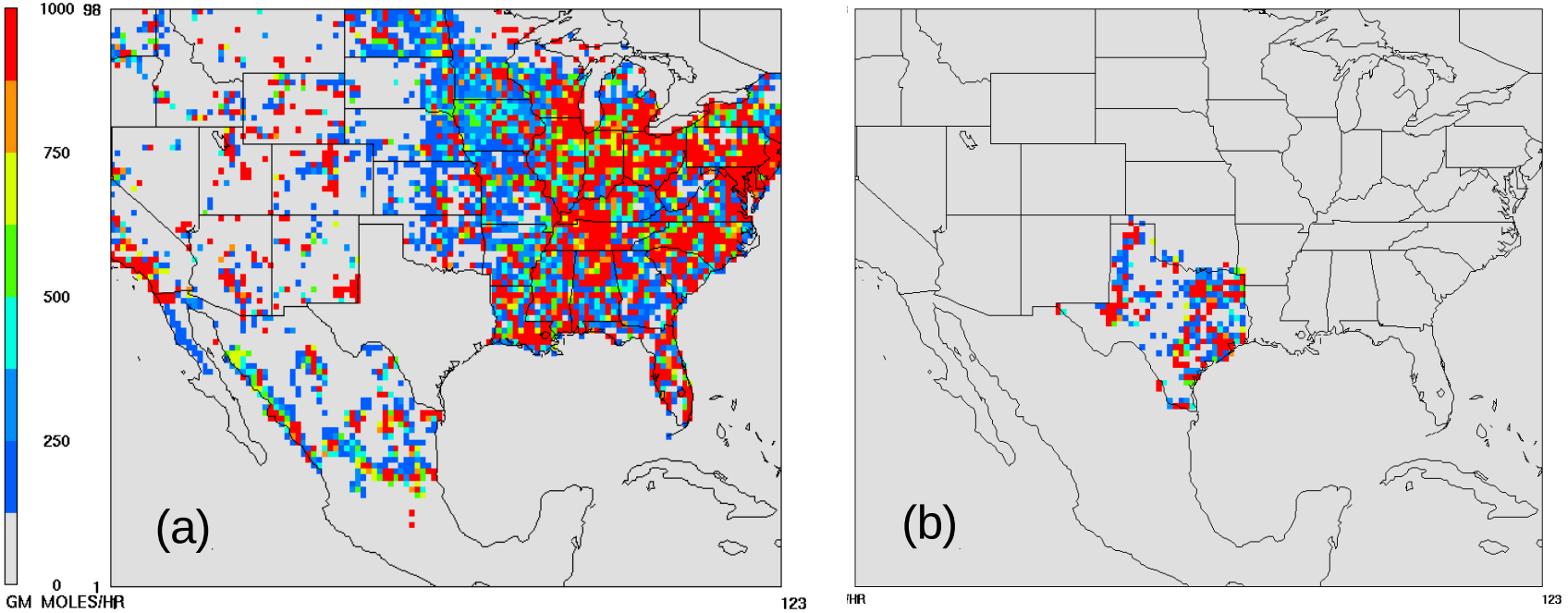

Figure 6-11. Example SO_2 emissions (moles/hr) for (a) the Texas "emissions out" scenario and (b) the Texas "emissions in" scenario.

It is important to investigate the equivalency of these two methods as either one could be regarded as a suitable approach for determining the impact of emissions from a source region on pollutant concentrations at a downwind receptor. Many processes within the model can be assumed to be linear and hence would yield the same results whether the "emissions out" or the "emissions in" inventory was used. These processes include, for example, dry deposition, as deposition fluxes scale in direct proportion to ambient concentrations. It is not obvious, however, that the rate of chemical transformation of sulfur dioxide to sulfate will respond in a linear fashion with regard to the "emissions out" and "emissions in" simulations. This is because the photochemistry that forms the oxidants that convert sulfur dioxide to sulfate is typically nonlinear. This includes the formation of hydroxyl for the gas-phase oxidation of sulfur dioxide and the formation of hydrogen peroxide and ozone for the aqueous-phase oxidation of sulfur dioxide. If there is a deficit in the concentration of available oxidants for converting sulfur dioxide to sulfate, i.e. an "oxidant limited" regime, then sulfate production will be sensitive to a change in the availability and distribution of oxidants. Sulfur dioxide acts as a sink for these oxidants, and the spatial distribution and total mass of sulfur dioxide within the model domain will be different between the "emissions out" and "emissions in" simulations. Oxidant levels should be greater in the "emissions in" scenarios as there is less total sulfur dioxide within the model domain to act as an oxidant sink and hence sulfate production should be enhanced relative to the "emissions out" scenarios.

The degree of linearity between the "emissions out" and "emissions in" sensitivity simulations is presented in Figure 6-12. Sulfate concentrations predicted at the K-Bar monitor for the original base simulation are shown in Figure 6-12a. Figures 6-12b through 6-12f show the difference in predicted sulfate contributions for the "emissions in" and "emissions out" simulations for the four major source regions, as well as the sulfate contribution from the boundary concentrations. For example, the time series shown in Figure 6-12b represents the sulfate contribution from Texas sources for the "emissions out" simulation, subtracted from the sulfate contribution from Texas sources for the "emissions in" simulation. If the predicted contributions are the same for the two sensitivity simulations, the difference will be zero and the model can be considered linear. Figures 6-12b through 6-12e show that this is generally the case, with the difference between the two sets of attributions at zero or very nearly zero for most of the four month simulation. A notable exception is evident, however, during the first half of October. During October 3–7 the maximum difference between the "emissions in" and "emissions out" contribution for both Texas and the eastern U.S. is approximately 0.5 $\mu g/m^3$, indicating an enhancement of sulfate formation for the "emissions in" simulation. A smaller enhancement also occurs during October 9–12, with the "emissions in" simulation yielding sulfate concentrations 0.3 $\mu g/m^3$ higher than the "emissions out" simulation. It is interesting to note that these periods coincide with enhanced transport from the oxidant-rich Houston area, as evidenced by the observed and predicted tracer time series shown in Figure 6-13.

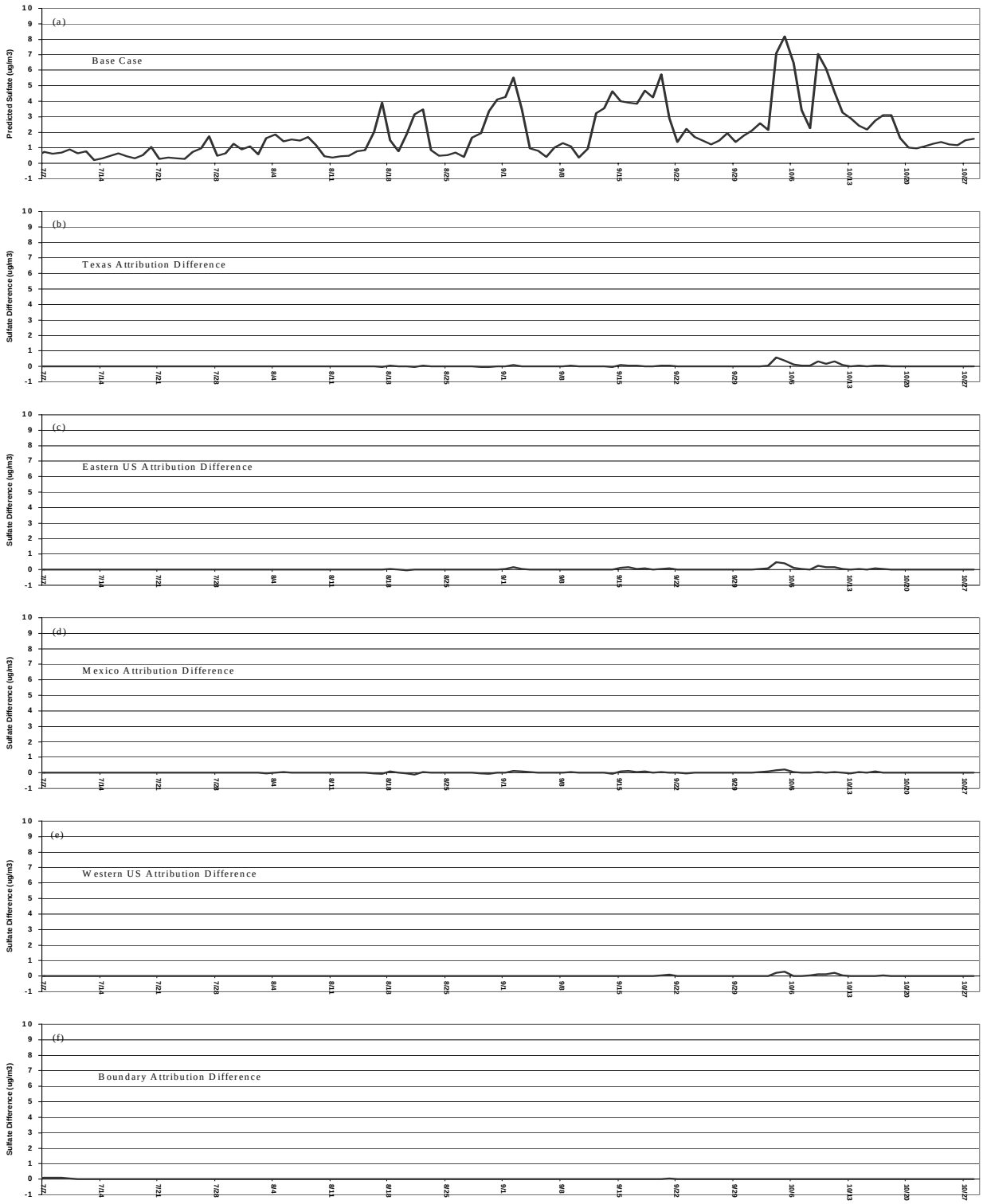

Figure 6-12. Degree of non-linearity between the "emissions out" and the "emissions in" simulations. (a) Predicted sulfate at K-Bar for the base emissions simulation. (b–e) Difference in predicted attributions for each source region (i.e. attribution from the "emissions out" simulation subtracted from the attribution from the "emissions in" simulation) for emission sources in (b) Texas, (c) the eastern U.S., (d) Mexico, (e) the western U.S., and (f) boundary concentrations.

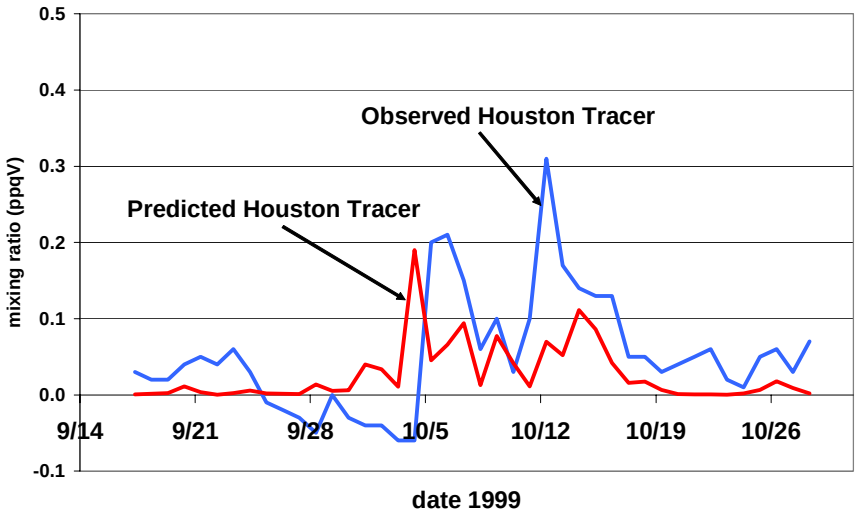

Figure 6-13. Predicted and observed Houston tracer concentrations measured at K-Bar.

From Figure 6-12 it is clear that the predicted attributions arising from the "emissions out" and the "emissions in" sensitivity simulations are very similar, with the "emissions in" simulations resulting in slightly enhanced sulfate production as expected. During the four month BRAVO period, the relative enhancements associated with the "emissions in" simulations were 2.8% for Mexican sources, 7.4% for Texas sources, 3.4% for eastern U.S. sources, 6.7% for western U.S. sources, and 4.2% for the boundary concentrations. This indicates that, in general, REMSAD behaves linearly with regard to the gross emission modifications presented in this chapter, and that attributions arising from the "emissions out" and "emissions in" sensitivity simulations are approximately equivalent. Therefore, to streamline the presentation of the following sulfate attribution section, only one set of attributions – the "emissions out" attributions – will be presented.

6.4 Sulfate Attribution Simulations

To determine the contribution of each of the four major regional source areas (Mexico, Texas, the eastern U.S., the western U.S.) on SO_4 concentrations at Big Bend NP, a series of REMSAD sensitivity simulations were evaluated with respect to the base emissions simulations. Additional emission sensitivity simulations were also conducted for evaluating the impact of several subregions and point sources, including northeastern and southeastern Texas, the Carbón I & II power plants near the Texas-Mexico border, and the Ohio River Valley. The influence of the GOCART-derived boundary concentration was also considered.

Example surface-level sulfate concentrations for the base emissions simulation and the emissions sensitivity simulations are shown in Figure 6-14 for a sulfate episode which occurred in mid-August of the BRAVO field study. The sulfate concentrations shown in Figures 6-14b–f are actually difference maps between the original base emissions simulation and the "emissions out" sensitivity simulation. In this particular example, observed and predicted sulfate concentrations at Big Bend NP were approximately 4 $\mu g/m^3$. During this period a region of elevated sulfate is evident in the base emissions simulation, ranging from 10 $\mu g/m^3$ to over 20 $\mu g/m^3$, and extends from eastern Texas toward Ohio and Pennsylvania (Figure 6-14a). Predicted sulfate concentrations are considerably lower over the western U.S., most of Mexico, and the Gulf of Mexico, with concentrations generally ranging between 0 $\mu g/m^3$ and 2 $\mu g/m^3$.

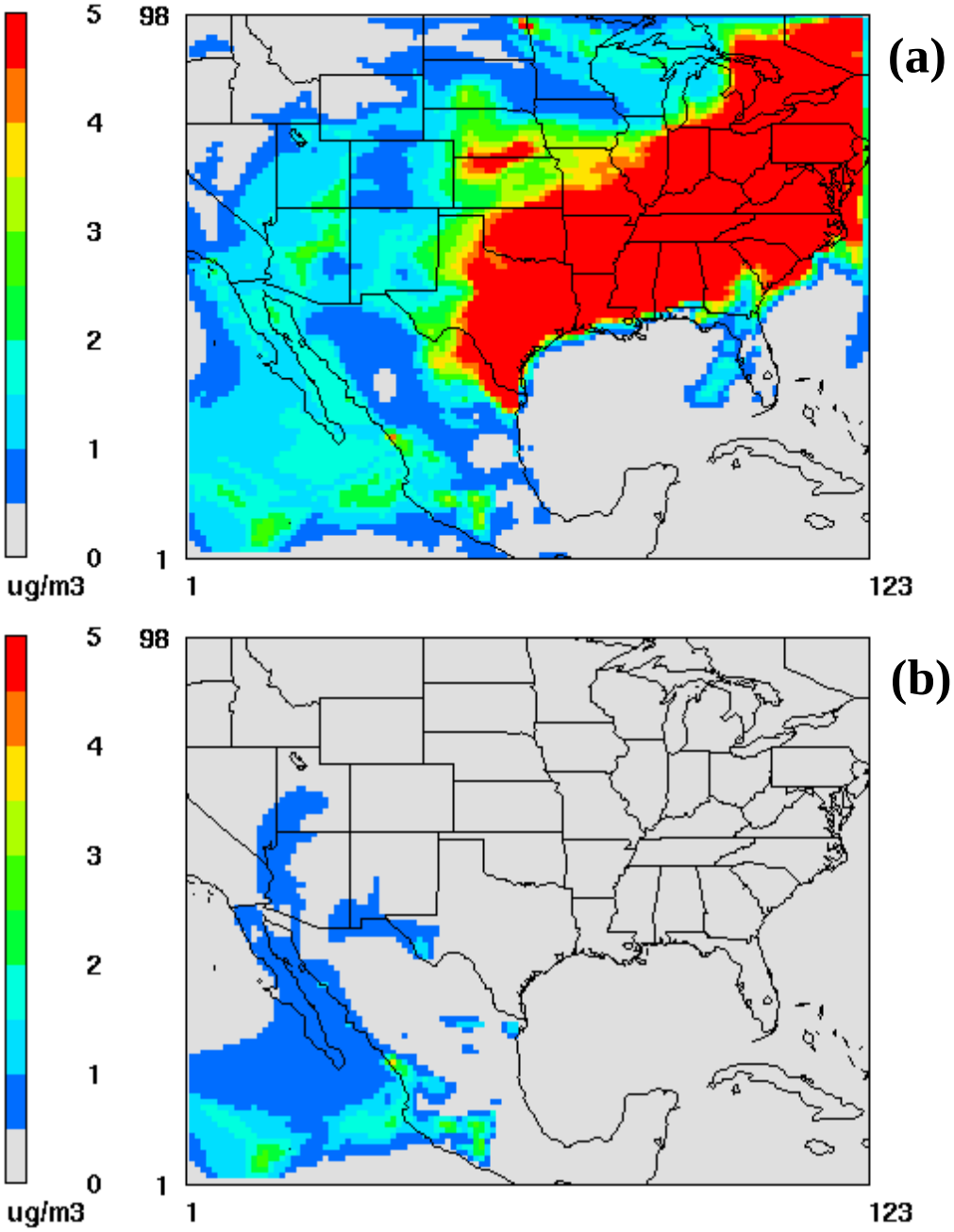
5
4
3
2
1
0
ug/m3
98
1
1
123
(a)
5
4
3
2
1
0
ug/m3
98
1
1
123
(b)

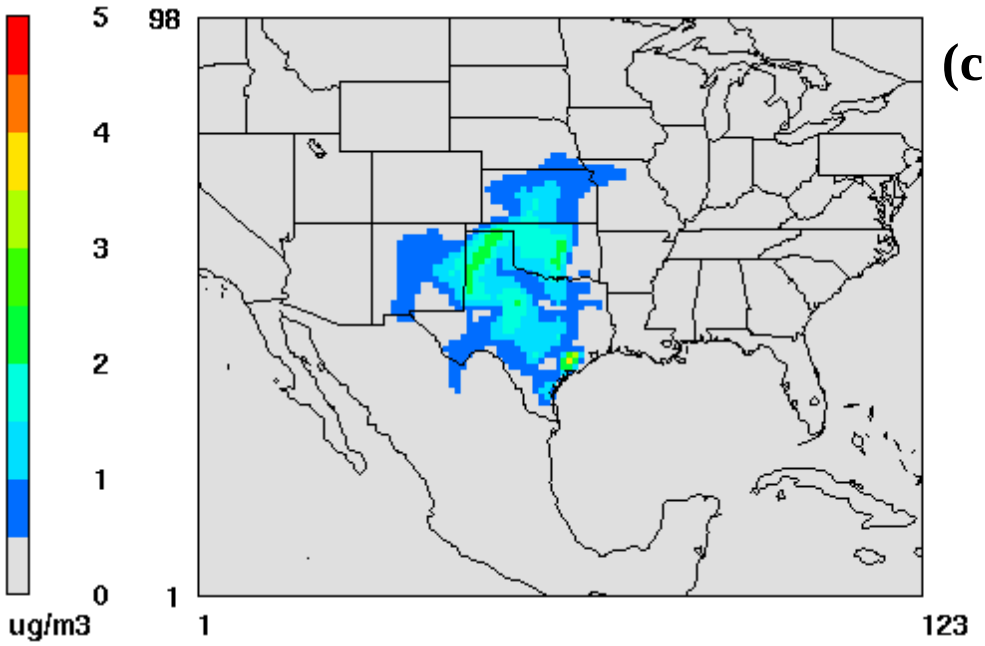

(c)

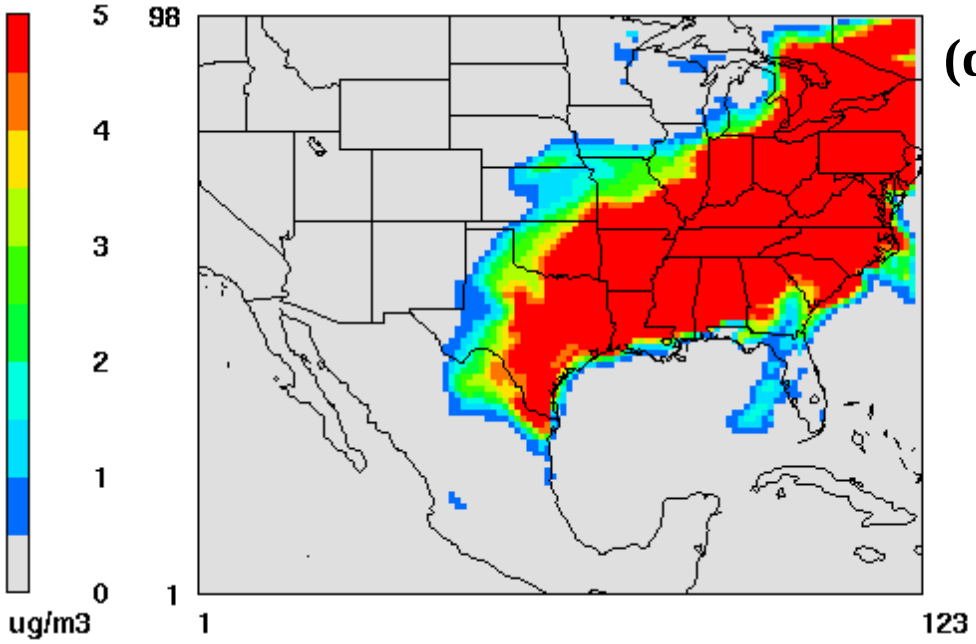

(d)

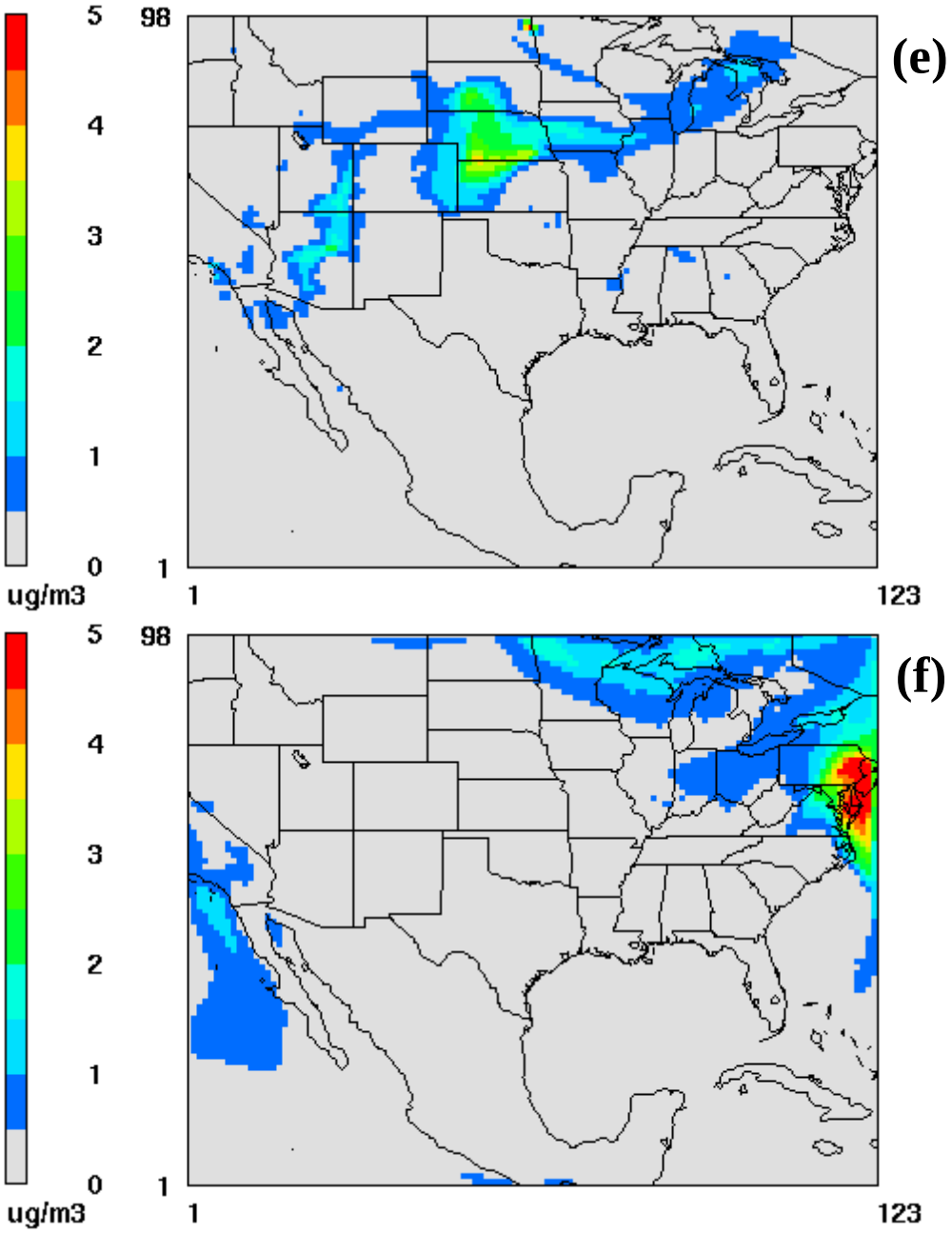

Figure 6-14. Surface sulfate concentrations (μg/m^3) on August 17, 1999, 1500 UTC, for the (a) base emissions simulation and contributions from the five emissions sensitivity simulations: (b) Mexico, (c) Texas, (d) the eastern U.S., (e) the western U.S., and (f) GOCART boundary concentrations.

The aggregation of sulfate contributions shown in the Figures 6-14b–f should approximate the base emissions scenario (Figure 6-14a). The contribution of each regional source (and the contribution of the concentrations specified at the model boundary) to total predicted sulfate levels for this period can be assessed by examining Figures 6-14b–f. For example, the magnitude of predicted sulfate attributed to eastern U.S. sources is clearly evident in Figure 6-14d, with sulfate concentrations exceeding 5 μg/m^3 in the mid- and eastern portions of the model domain. The dominance of eastern U.S. sources should be anticipated, given that approximately 77% of the SO_2 emitted within the REMSAD domain is from the eastern U.S.

Mexican sulfur sources, and in particular the Popocateptl volcano, result in elevated sulfate levels apparent off the western coast of Mexico, and the sulfate plume of the Carbón I & II power plants, in excess of 1.5 $\mu g/m^3$ near Big Bend NP, is evident along the western Texas-Mexico border (Figure 6-14b). Texas sulfur sources, located primarily in eastern Texas, are contributing to sulfate levels ranging from 0.5 $\mu g/m^3$ to 3 $\mu g/m^3$ which extend into western Texas and north into Oklahoma and Kansas (Figure 6-14c). Finally, for this particular period, the influence of western sulfur sources and sulfur concentrations specified at the model boundary is negligible on sulfate predicted at Big Bend NP (Figures 6-14e–f).

A notable aspect of Figures 6-14b–f is the extent to which a source region can influence predicted SO_4 concentrations downwind. For example, during this particular mid-August episode, sulfur emissions from eastern U.S. sources are contributing to sulfate concentrations in excess of 5 $\mu g/m^3$ in eastern Texas and extending into the border region of eastern Mexico (Figure 6-14d). Mexican sources are contributing approximately 1 $\mu g/m^3$ to predicted sulfate concentrations in southwestern Utah and western Arizona (Figure 6-14b), and similar levels are attributed to predicted sulfate in the Great Lakes region from western U.S. sources (Figure 6-14e). The impact of sulfur boundary concentrations specified by GOCART is primarily confined to the domain periphery, although a large contribution is clearly evident in proximity to the northeastern boundary (Figure 6-14f).

6.4.1 Simulated Sulfate Apportionment at Big Bend NP

Predicted source contributions at the K-Bar air quality monitor are shown in Figure 6-15 for each source region and emissions scenario combination for the four month BRAVO period. During July–August 1999 the largest contributor to sulfate at Big Bend NP is the eastern U.S., (42.1%), followed by Mexico (23.4%), Texas (16.1%), the western U.S. (9.1%), and the sulfur boundary concentrations derived from GOCART (6.7%). Figure 6-16 shows the overall and monthly sulfate concentrations predicted at Big Bend NP. As discussed in section 6.2, REMSAD under-predicts sulfate concentrations with respect to the average of the four month BRAVO period by approximately 20% (2.5 $\mu g/m^3$ observed vs. 2.0 $\mu g/m^3$ predicted). Possible explanations for this under-prediction include: 1) an under-estimation of SO_2 emissions for some regions, 2) errors in the simulated transport of SO_2 and SO_4, 3) slow SO_2 conversion rates, or 4) excessive wet or dry SO_4 deposition. The impact of these potential errors will influence the predicted source attributions. This bias, however, does not manifest itself consistently on a monthly basis. For example, predicted sulfate concentrations at Big Bend NP during July and August are approximately half the observed values (Figures 6-16b, c), while under-predictions during September are less acute (Figure 6-16d). Simulated sulfate during October, however, is over-predicted by approximately 25% (Figure 6-16e). This change in bias corresponds to different flow regimes that were evident during the BRAVO study. For example, trajectory analysis indicates that transport to Big Bend NP was predominately from Mexico during July and several periods in August. Transport patterns transitioned during September and October, however, yielding more influence from eastern U.S. and Texas sources during this period.

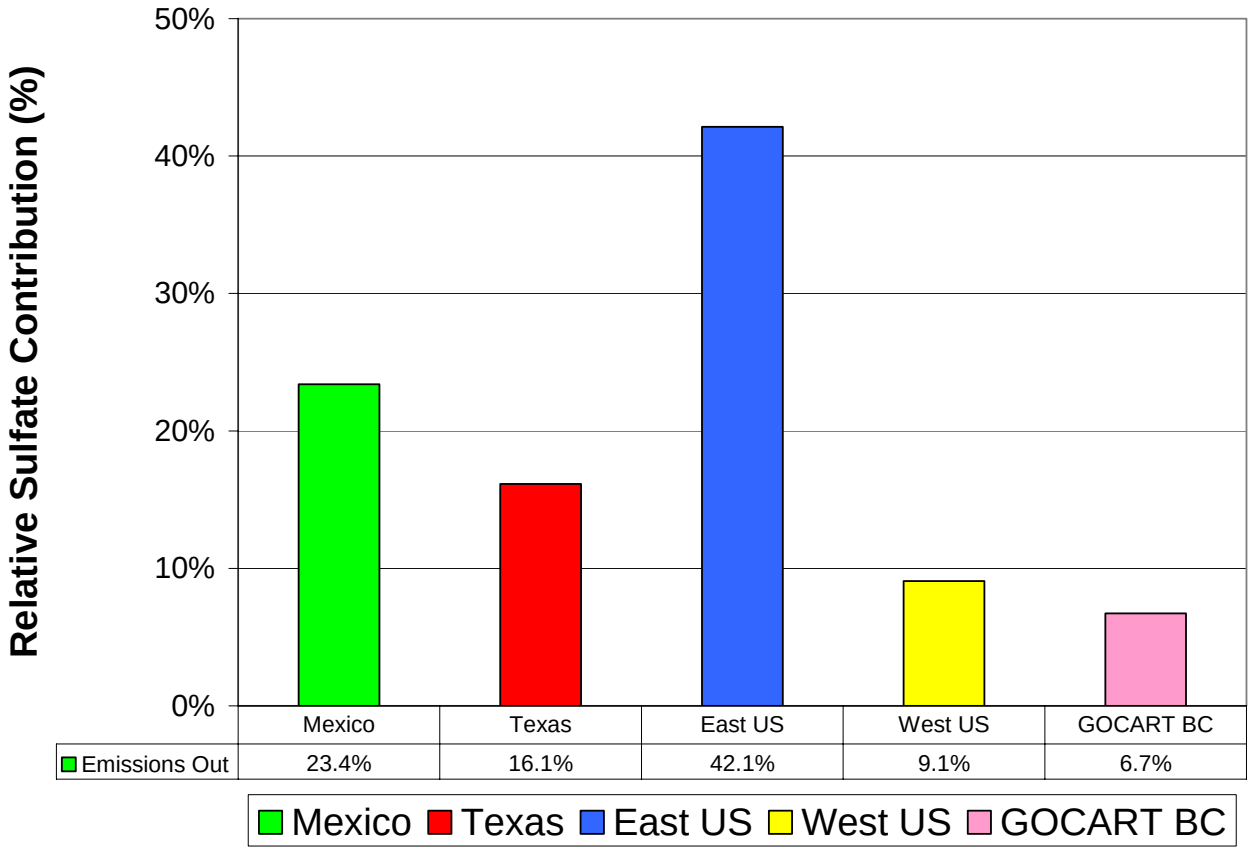

Figure 6-15. Four month average contributions to predicted sulfate at Big Bend NP from the "emissions out" sensitivity simulations for the four regional sources and the boundary concentrations.

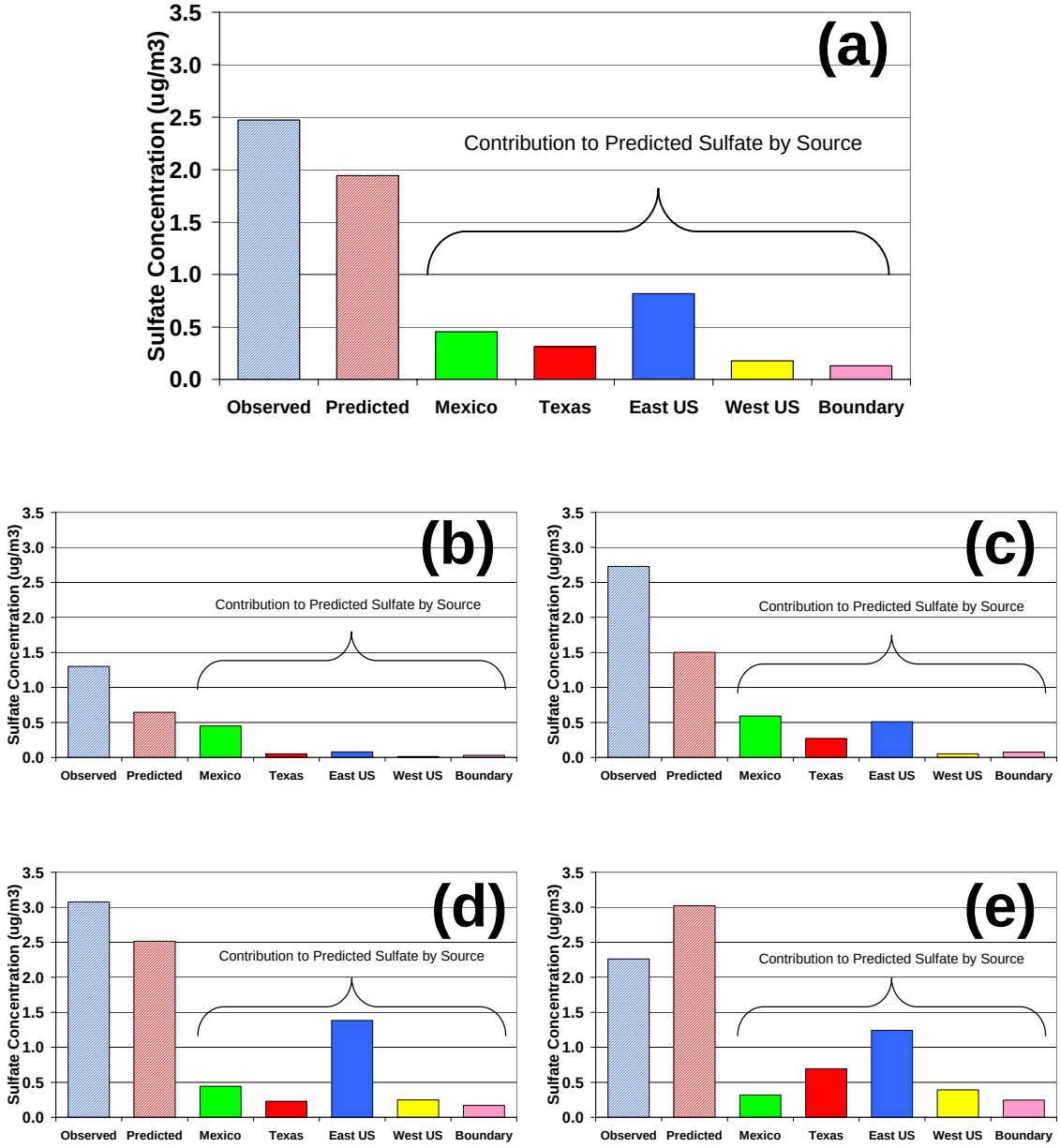

Figure 6-16. Observed sulfate, predicted sulfate, and predicted sulfate by source region at Big Bend NP for the "emissions out" simulations for (a) the entire BRAVO study period (July–October 1999), (b) July 1999, (c) August 1999, (d) September 1999, and (e) October 1999.

Relative sulfate attributions are presented Figures 6-17. Again, the overall relative attribution is significantly different than the monthly attributions, with a transition from a Mexican-dominated influence in the early part of the study (Figures 6-17b,c) to a regime where eastern U.S. sources, and to a lesser extent, Texas sources, are prevalent. For example, Mexican contributions to Big Bend NP sulfate drop from 70% in July (Figure 6-17b) to only 11% in October (Figure 6-17e), while eastern U.S. sources rise from 12% (Figure 6-17b) to 55% in September (Figure 6-17d) and 41% in October (Figure 6-17e).

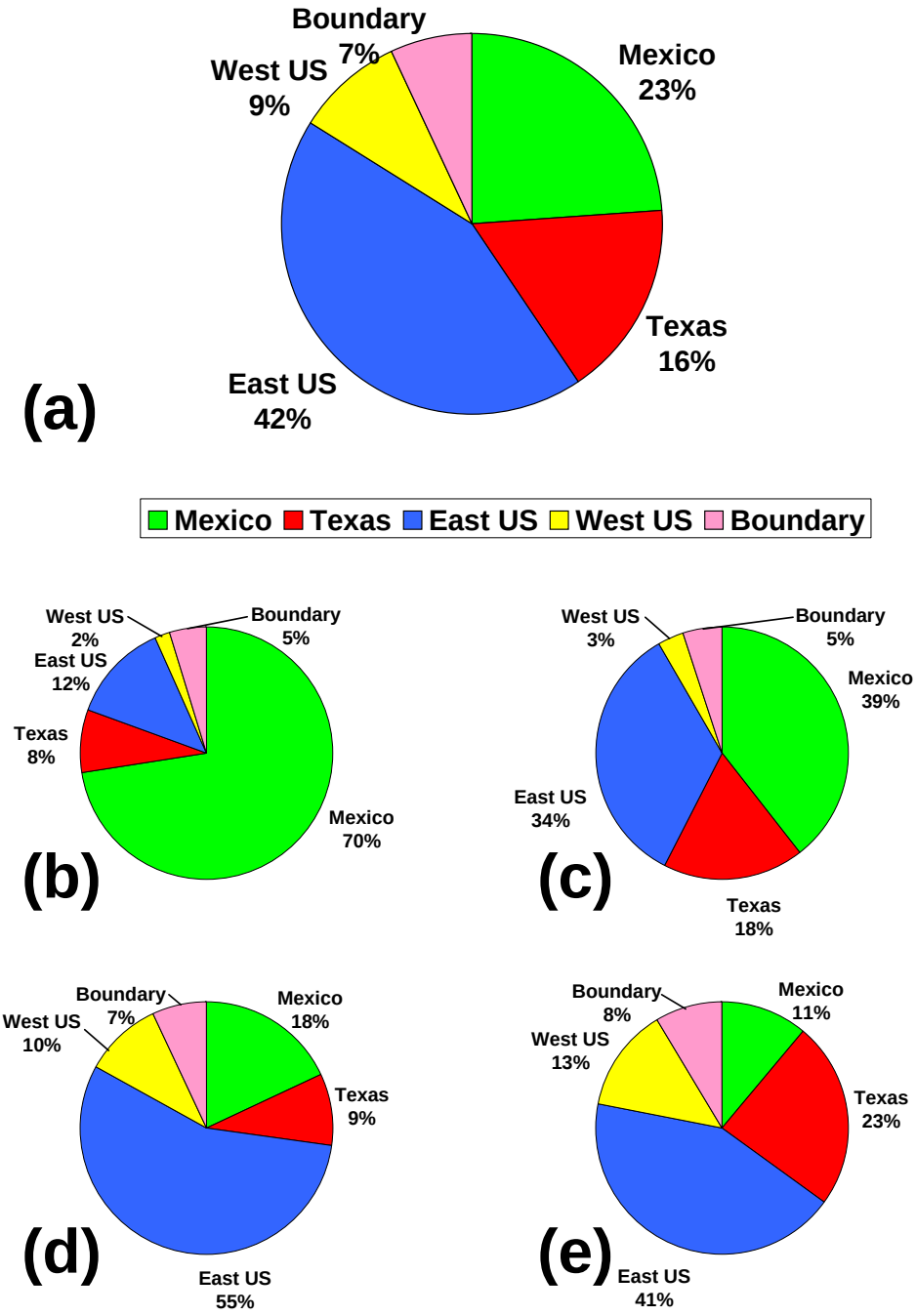

Figure 6-17. Relative contribution of predicted sulfate to Big Bend NP by source region for the "emissions out" simulations for (a) the entire BRAVO study period (July–October 1999), (b) July 1999, (c) August 1999, (d) September 1999, and (e) October 1999.

SO_4 source attributions at the K-Bar monitor can also be examined on a daily basis, as shown in Figures 6-18 and 6-19. Figure 6-18 displays the absolute SO_4 contribution for each source region, and Figure 6-19 illustrates the relative contribution for each source region. During July and the first half of August, transport is predominantly from Mexico. Predicted SO_4 concentrations during this period are lower than observed. Although the absolute contribution

from Mexican sources may be quite small during this period (< 1 μg/m^3), these contributions will have a disproportionate impact on visibility since SO_4 concentrations within Big Bend NP are relatively low during this time. Small incursions of SO_4 from western U.S. sources are evident from July through mid-September.

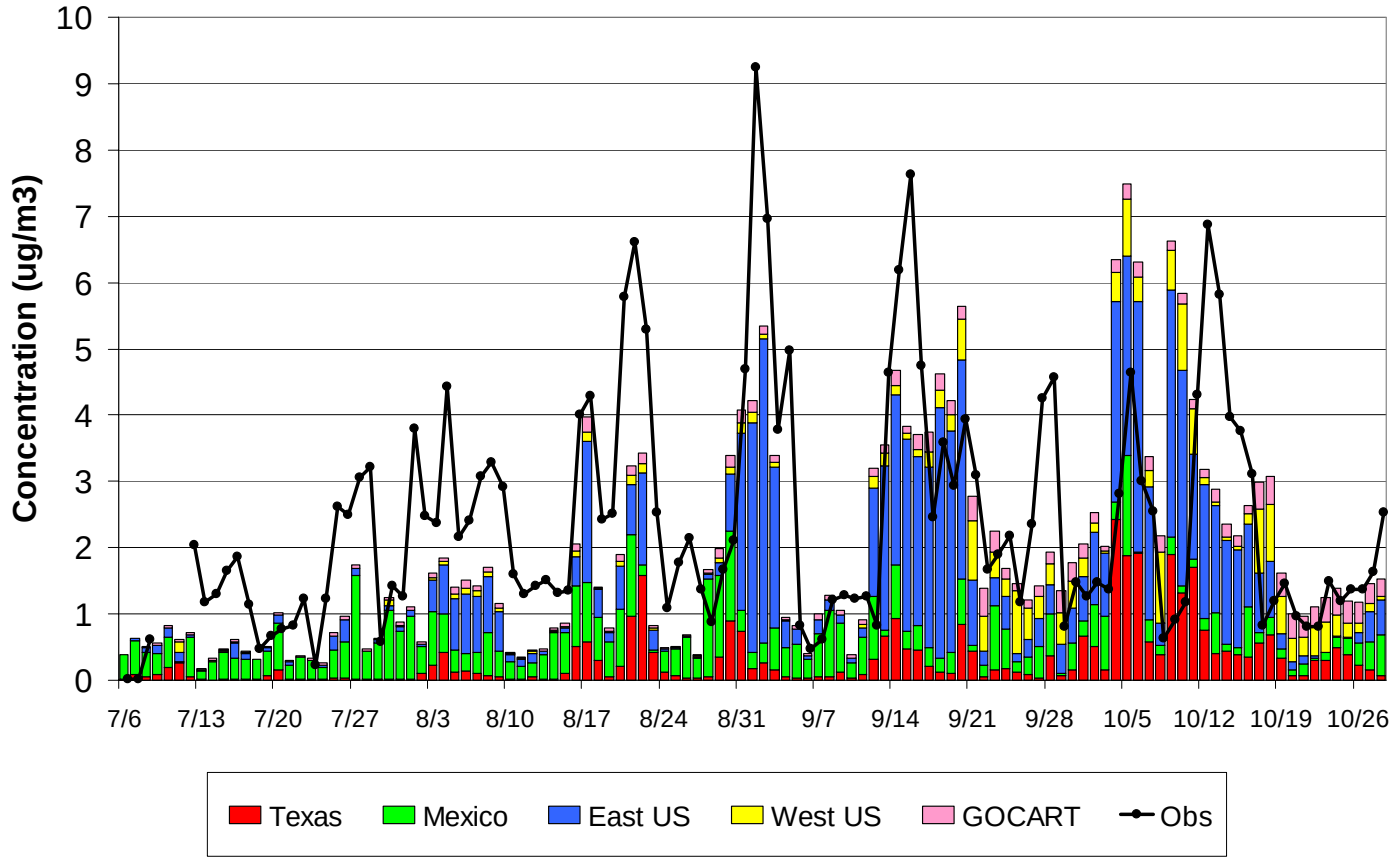

Figure 6-18. Daily absolute attribution of sulfate to Big Bend NP.

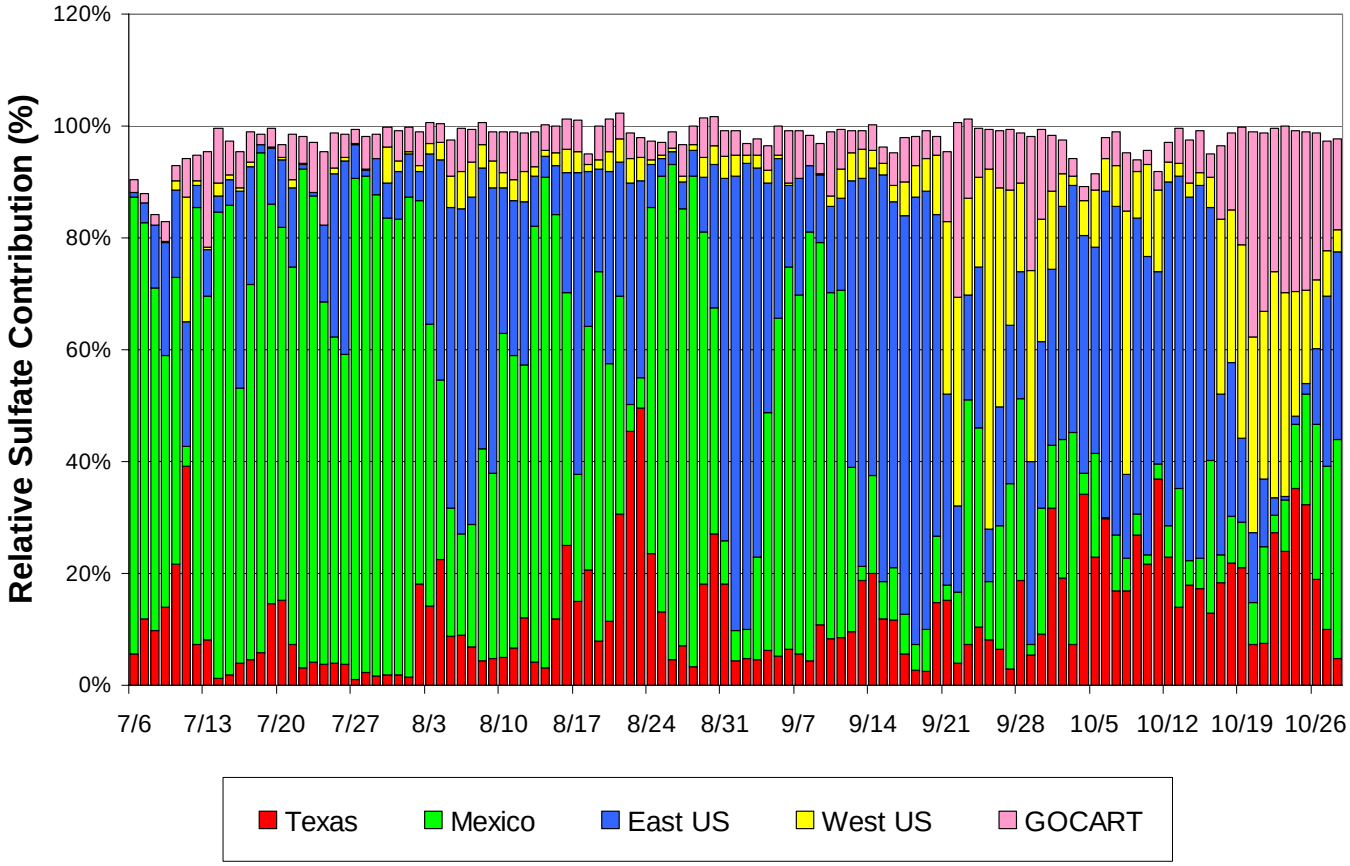

Figure 6-19. Daily relative attribution of sulfate to Big Bend NP.

From mid-August onward the high SO_4 episodes show a major component of eastern U.S. SO_4. This is especially evident in the two September SO_4 episodes, when the relative proportion of eastern U.S. SO_4 can exceed 80%. It is also notable that during these two episodes the predicted SO_4 concentrations are significantly lower than the observed values. Mexican emissions dominate the relatively clean period between these two September episodes. The two October SO_4 episodes also show a major contribution from eastern U.S. sources, but Texas sources, and to a lesser extent Mexican and western U.S. sources, also have a considerable impact. In contrast to the September SO_4 episodes, there is a substantial over-prediction of the October 5 SO_4 peak, and the subsequent peak (observed on October 12) appears to be shifted forward by three days. The intervening periods between the late September and October SO_4 episodes show a more evenly mixed distribution among all four source regions.

In addition to the four major source regions discussed above, sulfate apportionment at Big Bend NP can also be refined to smaller subregions, as shown in Figure 6-20. In proximity to Big Bend NP are the subregions of northeast and southeast Texas, with SO_2 emissions of 506,000 tons/year and 445,000 tons/year, respectively, and the Carbón I & II power plants, with SO_2 emissions of 152,000 ton/year. Also, three subregions within the eastern U.S. are considered: (1) Louisiana and southern Mississippi, with SO_2 emissions of 935,000 tons/year, (2) Missouri, Arkansas, southern Illinois, northern Mississippi, and portions of Indiana, Kentucky and Tennessee, with SO_2 emissions of 2,812,000 tons/year, and (3) an "East Central" region consisting of Virginia, North Carolina, South Carolina, West Virginia, northern Georgia and Alabama, eastern Kentucky and Tennessee, southern Indiana and Ohio, Maryland, Delaware, and southern New Jersey, with emissions of 5,514,000 tons/year. Emission sensitivity simulations were performed for these subregions, and contributions are shown in Table 6-4. Of these subregions, the Carbón I & II power plants have the largest impact at Big Bend NP, contributing approximately 14% of the total sulfate. Northeast and southeast Texas contribute 5% and 9%, respectively, and contributions from the three subregions within the eastern U.S. range between 9% and 13%.

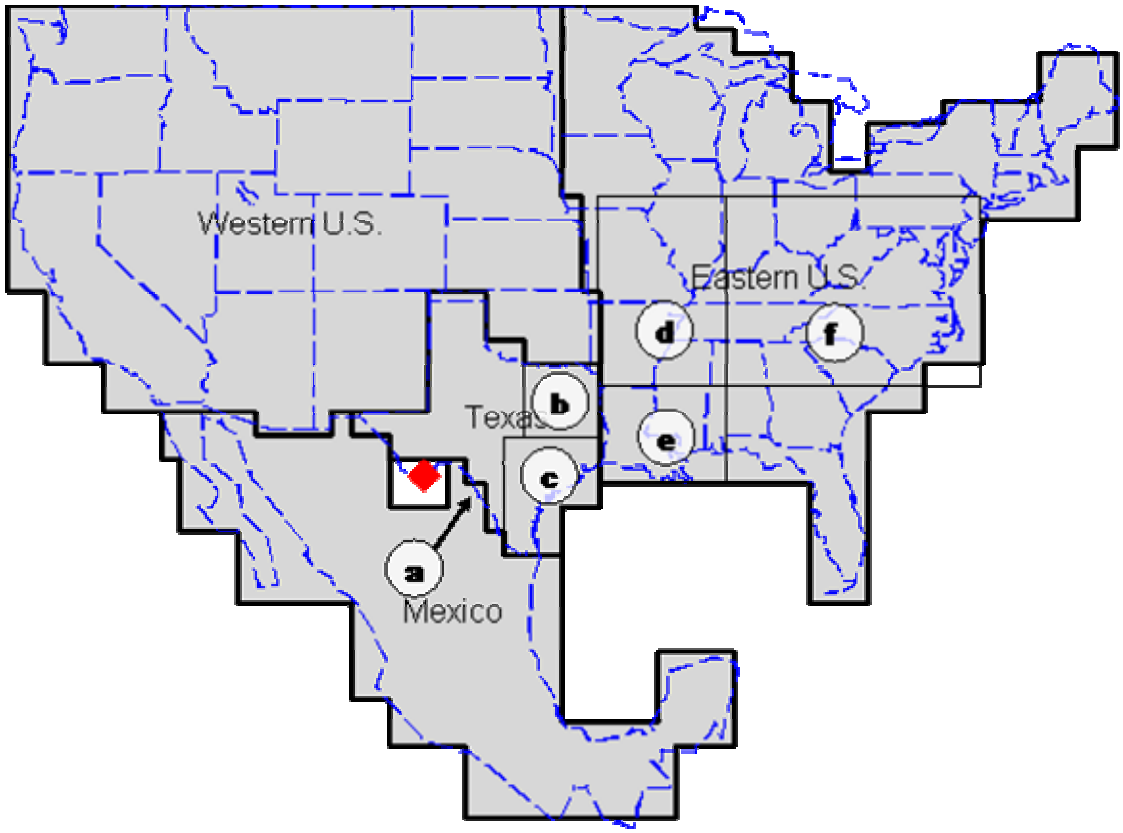

Figure 6-20. Domain map, showing the (a) Carbón I & II power plants and the subregions of (b) northeastern Texas, (c) southeastern Texas, (d) Missouri/Illinois/Arkansas, (e) Louisiana/Mississippi, and (f) "East Central".

Table 6-4. Predicted subregional contributions to Big Bend NP sulfate.

	Regional Contribution	Subregional Contribution
	(%)	(%)
Mexico (all)	**23.4%**	
Carbón I & II		13.7%
Rest of Mexico		9.7%
Texas (all)	**16.1%**	
NE Texas		5.3%
SE Texas		8.6%
Western Texas		2.2%
Eastern U.S. (all)	**42.1%**	
Louisiana/Mississippi		9.0%
"East Central"		13.2%
Missouri/Illinois/Arkansas		12.7%
Rest of Eastern U.S.		7.2%
Western U.S. (all)	**9.1%**	
Boundary Concentrations	**6.7%**	
Total Contribution	**97.5%**	

6.4.2 Simulated Sulfate Apportionment at the BRAVO Monitors

The predicted and observed sulfate concentrations and the contribution of the major source regions to the predicted sulfate were examined for each site by aggregating over each month (Tables 6-5 to 6-8, Figure 6-21) and for each day by aggregating over large regions within Texas (Figure 6-22). As shown in Figures 6-21 and 6-23, during July REMSAD underestimated the sulfate at all of the monitoring sites. This is most severe in southern Texas where the average sulfate was underestimated by more than a factor of 2 over all sites (Figure 6-23b) and a factor of 4 to 5 along the Texas-Mexico Border. Western Texas, around the Big Bend region, was also underestimated by about a factor of 2. During July, Mexico contributed more than half of the predicted sulfate at most sites in west Texas and about 75% of the sulfate at Big Bend. In southern Texas, eastern U.S. and Texas sources contributed equally to the predicted sulfate, while Texas sources were the largest contributor to eastern Texas sulfate.

Table 6-5. The average July source attribution for all BRAVO monitoring sites. All units are in µg/m^3.

Region/Site	Western U.S.	Mexico	Texas	Eastern U.S.	Pred SO_4	Obs SO_4
West Texas						
Amistad	0.00	0.56	0.12	0.16	0.92	2.01
Esperanza	0.15	0.94	0.06	0.19	1.41	2.11
Fort Lancaster	0.00	0.64	0.10	0.20	0.99	2.14
Fort Stockton	0.07	0.63	0.12	0.14	1.05	2.03
Guadalupe Mtns						

K-Bar	0.01	0.47	0.03	0.07	0.63	1.30
Langtry	0.01	0.62	0.17	0.17	1.04	2.86
Marathon	0.05	0.66	0.10	0.13	1.00	1.80
McDonald Obs	0.13	0.85	0.05	0.13	1.20	1.62
Monahans Sandhills	0.08	0.53	0.27	0.18	1.16	2.00
Persimmon Gap	0.04	0.56	0.11	0.10	0.88	1.54
Presidio	0.14	0.83	0.03	0.15	1.22	1.58
Sanderson	0.03	0.66	0.14	0.15	1.04	2.59
San Vicente	0.01	0.45	0.05	0.08	0.65	1.38
Average	0.05	0.65	0.11	0.14	1.01	1.92
South Texas						
Aransas	0.01	0.00	0.09	0.73	0.90	2.20
Brackettville	0.00	0.09	0.19	0.24	0.57	1.42
Eagle Pass	0.00	0.15	0.08	0.18	0.48	1.62
Falcon Dam	0.00	0.21	0.02	0.13	0.41	3.09
Laguna Atascosa	0.00	0.01	0.02	0.20	0.28	1.61
Lake Corpus Christi	0.01	0.01	0.21	0.49	0.78	2.27
Laredo	0.00	0.18	0.03	0.15	0.42	1.68
Padre Island	0.01	0.03	0.06	0.64	0.80	2.61
Pleasanton	0.00	0.03	0.55	0.30	0.97	1.96
San Bernard	0.02	0.01	0.39	0.79	1.27	2.26
Average	0.01	0.15	0.15	0.34	0.71	2.00
East Texas						
Big Thicket	0.02	0.01	1.12	0.95	2.16	3.13
Center	0.03	0.02	1.57	1.13	2.81	3.43
Everton Ranch	0.01	0.01	0.29	0.63	1.00	3.37
Hagerman	0.01	0.02	1.55	0.54	2.17	2.55
LBJ NHS	0.00	0.01	1.23	0.32	1.66	2.48
Purtis Creek	0.02	0.01	1.49	0.60	2.18	2.72
Somerville Lake	0.01	0.01	1.13	0.59	1.86	2.14
Stephenville	0.01	0.01	0.69	0.31	1.06	1.99
Stillhouse Lake	0.01	0.00	1.45	0.53	2.10	2.26
Wright Patman	0.04	0.02	3.03	0.81	3.96	5.35
Average	0.02	0.02	1.17	0.63	1.91	2.81
Other						
Fort McKavett	0.03	0.11	0.63	0.28	1.16	1.70
Lake Colorado City	0.00	0.41	0.32	0.17	0.95	1.97
Wichita Mtns						
Average	0.01	0.06	1.18	0.49	1.82	2.67

Table 6-6. The average August source attribution for all BRAVO monitoring sites. All units are in µg/m^3.

Region/Site	Western U.S.	Mexico	Texas	Eastern U.S.	Pred SO_4	Obs SO_4
West Texas						
Amistad	0.06	0.30	0.54	0.91	1.91	3.25
Esperanza	0.14	0.59	0.36	0.45	1.65	2.09
Fort Lancaster	0.08	0.22	0.65	0.99	2.04	2.81
Fort Stockton	0.07	0.46	0.42	0.66	1.69	2.86
Guadalupe Mtns	0.15	0.46	0.44	0.35	1.52	2.28
K-Bar	0.05	0.59	0.27	0.51	1.50	2.73
Langtry	0.07	0.30	0.54	0.95	1.97	3.58
Marathon	0.06	0.46	0.36	0.60	1.57	2.74
McDonald Obs	0.08	0.51	0.36	0.52	1.56	2.47
Monahans Sandhills	0.08	0.40	0.70	0.82	2.10	3.24
Persimmon Gap	0.06	0.55	0.34	0.57	1.61	3.13
Presidio	0.05	0.61	0.26	0.48	1.48	2.21
Sanderson	0.06	0.42	0.45	0.71	1.73	3.31
San Vicente	0.05	0.55	0.29	0.54	1.51	2.90
Average	0.08	0.46	0.43	0.65	1.70	2.83
South Texas						
Aransas	0.08	0.04	0.40	2.12	2.77	3.60
Brackettville	0.07	0.05	0.64	1.11	1.98	3.52
Eagle Pass	0.06	0.05	0.42	1.04	1.68	2.79
Falcon Dam	0.05	0.20	0.23	0.94	1.49	2.58
Laguna Atascosa	0.06	0.03	0.18	1.22	1.56	2.56
Lake Corpus Christi	0.08	0.05	0.63	1.59	2.46	2.42
Laredo	0.06	0.11	0.37	1.15	1.79	2.50
Padre Island	0.06	0.02	0.10	1.39	1.66	3.51
Pleasanton	0.08	0.07	0.96	1.62	2.84	3.34
San Bernard	0.09	0.04	0.83	2.31	3.41	3.60
Average	0.07	0.14	0.46	1.31	2.07	3.01
East Texas						
Big Thicket	0.12	0.04	0.65	3.59	4.59	4.35
Center	0.16	0.03	0.61	5.09	6.15	5.56
Everton Ranch	0.08	0.05	0.85	1.69	2.79	3.53
Hagerman	0.24	0.04	1.11	3.59	5.26	5.47
LBJ NHS	0.10	0.05	1.26	1.72	3.25	3.88
Purtis Creek	0.20	0.03	1.10	3.49	5.06	5.58
Somerville Lake	0.13	0.04	1.05	2.69	4.07	4.31
Stephenville	0.16	0.05	1.12	2.27	3.77	4.67
Stillhouse Lake	0.14	0.04	1.13	2.55	4.03	4.86
Wright Patman	0.23	0.04	1.01	6.24	7.87	6.19
Average	0.14	0.05	0.93	3.04	4.36	4.58
Other						
Fort McKavett	0.10	0.09	0.98	1.33	2.61	3.20

Lake Colorado City	0.14	0.14	1.06	1.31	2.76	3.35
Wichita Mtns	0.41	0.04	1.01	2.99	4.72	4.55
Average	0.17	0.06	1.05	2.74	4.21	4.51

Table 6-7. The average September source attribution for all BRAVO monitoring sites. All units are in µg/m^3.

Region/Site	**Western U.S.**	**Mexico**	**Texas**	**Eastern U.S.**	**Pred SO_4**	**Obs SO_4**
West Texas						
Amistad	0.21	0.56	0.58	2.42	4.01	3.69
Esperanza	0.40	0.44	0.40	0.86	2.28	2.05
Fort Lancaster	0.28	0.50	0.69	1.87	3.58	3.87
Fort Stockton	0.31	0.52	0.53	1.57	3.15	2.96
Guadalupe Mtns	0.34	0.38	0.45	1.08	2.44	2.27
K-Bar	0.25	0.44	0.23	1.41	2.52	3.08
Langtry	0.23	0.62	0.59	2.20	3.88	4.04
Marathon	0.29	0.53	0.41	1.54	2.97	3.22
McDonald Obs	0.34	0.42	0.41	1.18	2.53	2.29
Monahans Sandhills	0.33	0.49	0.68	1.60	3.32	3.63
Persimmon Gap	0.28	0.53	0.37	1.53	2.91	3.25
Presidio	0.28	0.42	0.25	1.25	2.38	2.84
Sanderson	0.28	0.58	0.53	1.84	3.45	3.27
San Vicente	0.25	0.44	0.23	1.41	2.52	3.09
Average	0.29	0.49	0.45	1.55	3.00	3.11
South Texas						
Aransas	0.12	0.02	0.39	3.93	4.78	4.12
Brackettville	0.18	0.04	0.65	2.74	3.89	3.67
Eagle Pass	0.21	0.06	0.73	3.41	4.70	3.54
Falcon Dam	0.14	0.22	0.35	3.52	4.47	3.69
Laguna Atascosa	0.11	0.02	0.30	3.96	4.65	3.80
Lake Corpus Christi	0.13	0.02	0.49	3.97	4.91	3.78
Laredo	0.16	0.11	0.48	3.60	4.60	3.92
Padre Island	0.15	0.03	0.53	4.53	5.57	4.24
Pleasanton	0.16	0.03	0.92	3.96	5.38	4.38
San Bernard	0.10	0.01	0.67	3.87	4.98	4.61
Average	0.17	0.12	0.52	3.37	4.45	3.83
East Texas						
Big Thicket	0.10	0.01	0.35	4.21	5.04	4.22
Center	0.09	0.01	0.28	3.47	4.20	3.49
Everton Ranch	0.16	0.02	0.80	3.50	4.79	4.00
Hagerman	0.16	0.02	0.91	1.95	3.39	3.57
LBJ NHS	0.19	0.03	1.10	2.76	4.35	3.22
Purtis Creek	0.11	0.01	1.04	2.64	4.14	4.04
Somerville Lake	0.14	0.02	0.76	2.92	4.16	3.52
Stephenville	0.19	0.05	0.85	2.24	3.64	3.38
Stillhouse Lake	0.16	0.02	0.88	2.72	4.09	3.67
Wright Patman	0.09	0.01	0.62	3.09	4.22	3.67

Average	0.14	0.03	0.73	3.06	4.29	3.77
Other						
Fort McKavett	0.24	0.15	0.80	2.09	3.53	3.08
Lake Colorado City	0.40	0.28	0.84	1.68	3.46	3.03
Wichita Mtns	0.38	0.09	0.88	1.67	3.36	2.54
Average	0.20	0.06	0.85	2.53	3.95	3.46

Table 6-8. The average October source attribution for all BRAVO monitoring sites. All units are in µg/m^3.

Region/Site	Western U.S.	Mexico	Texas	Eastern U.S.	Pred SO_4	Obs SO_4
West Texas						
Amistad	0.42	0.46	0.78	2.57	4.60	3.00
Esperanza	0.47	0.25	0.51	0.65	2.13	1.68
Fort Lancaster	0.46	0.39	0.74	2.17	4.11	2.68
Fort Stockton	0.46	0.33	0.71	1.40	3.22	2.14
Guadalupe Mtns	0.54	0.19	0.51	0.64	2.15	1.56
K-Bar	0.39	0.32	0.69	1.32	3.02	2.26
Langtry	0.44	0.45	0.75	2.34	4.35	3.26
Marathon	0.44	0.31	0.69	1.41	3.15	2.22
McDonald Obs	0.44	0.30	0.61	0.91	2.54	1.67
Monahans Sandhills	0.49	0.38	0.84	1.68	3.73	2.78
Persimmon Gap	0.44	0.30	0.70	1.45	3.19	2.50
Presidio	0.42	0.36	0.70	1.12	2.89	1.96
Sanderson	0.46	0.38	0.72	1.90	3.79	2.77
San Vicente	0.37	0.34	0.74	1.43	3.16	2.51
Average	0.45	0.34	0.69	1.50	3.29	2.36
South Texas						
Aransas	0.15	0.03	0.94	4.38	5.80	3.67
Brackettville	0.37	0.14	0.83	2.92	4.63	2.72
Eagle Pass	0.35	0.18	0.83	2.92	4.64	2.86
Falcon Dam	0.20	0.17	0.94	2.86	4.46	2.85
Laguna Atascosa	0.13	0.03	0.71	2.93	4.06	3.02
Lake Corpus Christi	0.17	0.06	1.23	3.74	5.53	3.39
Laredo	0.25	0.20	1.06	3.12	4.96	3.11
Padre Island	0.15	0.03	1.05	3.91	5.45	3.60
Pleasanton	0.24	0.08	1.30	3.70	5.69	3.17
San Bernard	0.12	0.02	0.79	4.75	5.99	4.12
Average	0.24	0.13	0.93	3.18	4.81	3.12
East Texas						
Big Thicket	0.13	0.02	0.32	5.57	6.37	4.30
Center	0.14	0.01	0.28	5.33	6.12	3.04
Everton Ranch	0.24	0.04	1.17	4.20	6.04	3.19
Hagerman	0.38	0.02	0.78	3.99	5.55	3.40
LBJ NHS	0.32	0.04	1.03	3.38	5.14	2.68
Purtis Creek	0.26	0.01	0.99	4.13	5.79	3.52
Somerville Lake	0.22	0.02	1.10	4.49	6.20	3.65

Stephenville	0.37	0.03	0.82	3.41	4.99	2.68
Stillhouse Lake	0.29	0.02	1.15	4.06	5.90	3.23
Wright Patman	0.19	0.01	0.67	4.79	6.04	3.02
Average	0.24	0.03	0.84	4.27	5.74	3.33
Other						
Fort McKavett	0.43	0.11	0.78	2.63	4.29	2.21
Lake Colorado City	0.50	0.27	0.81	2.24	4.20	2.24
Wichita Mtns						
Average	0.31	0.06	0.92	3.78	5.44	3.01

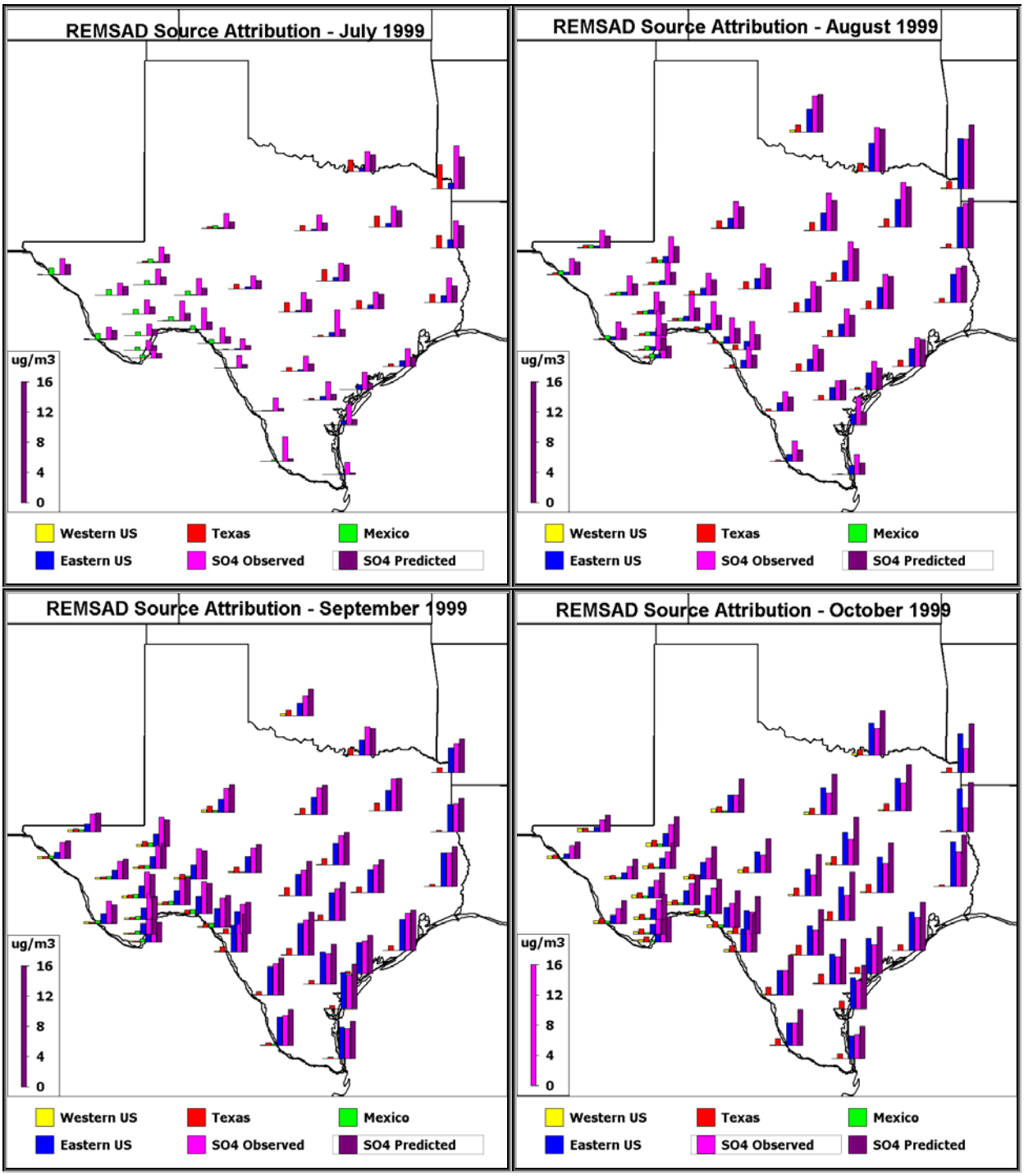

Figure 6-21. The average source attribution to each BRAVO monitoring site for each month during BRAVO. The average observed sulfate and REMSAD predicted sulfate are also included. Only days with a valid measured sulfate concentration were used in each site's averages.

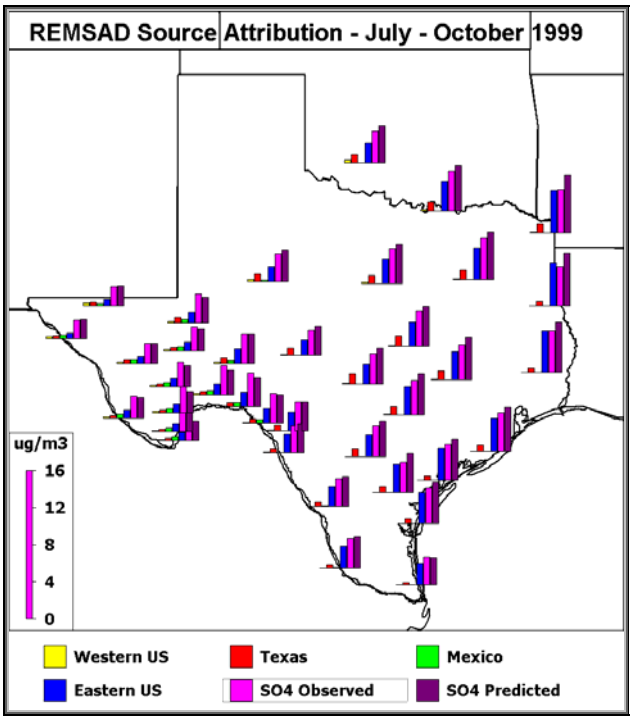

Figure 6-22. The average source attribution to each BRAVO monitoring site over the entire BRAVO period. Only days with a valid measured sulfate concentration were used in each site's averages. The boxes show the west, south, and east Texas aggregation regions used in Figure 23.

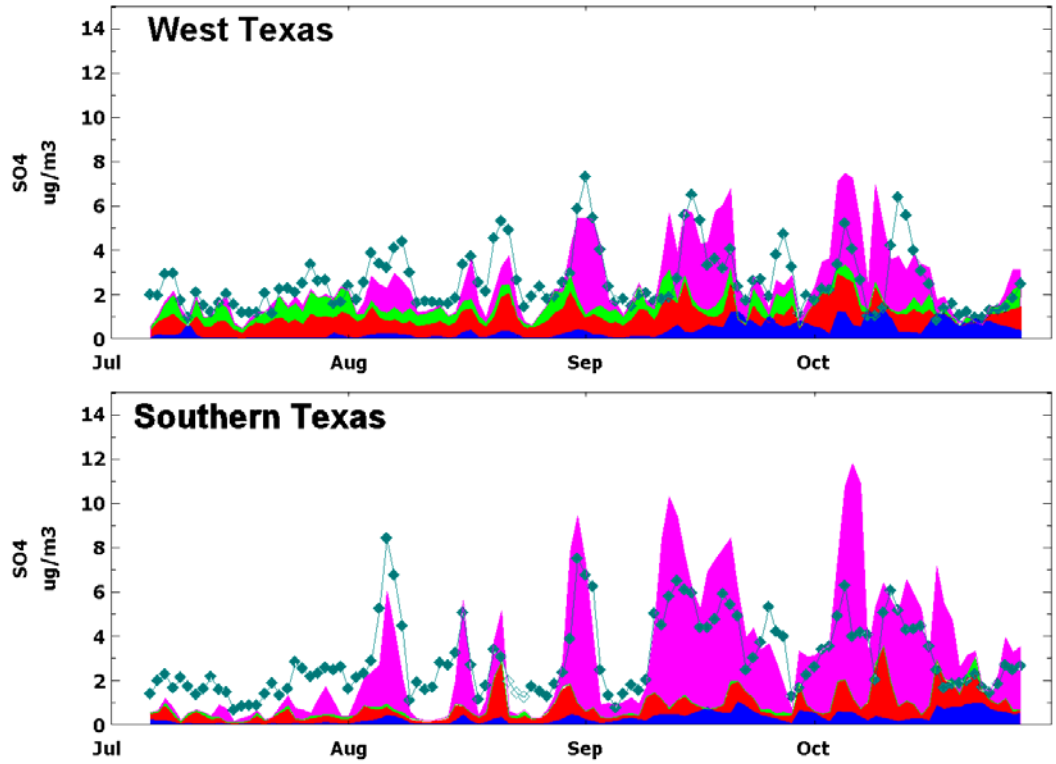

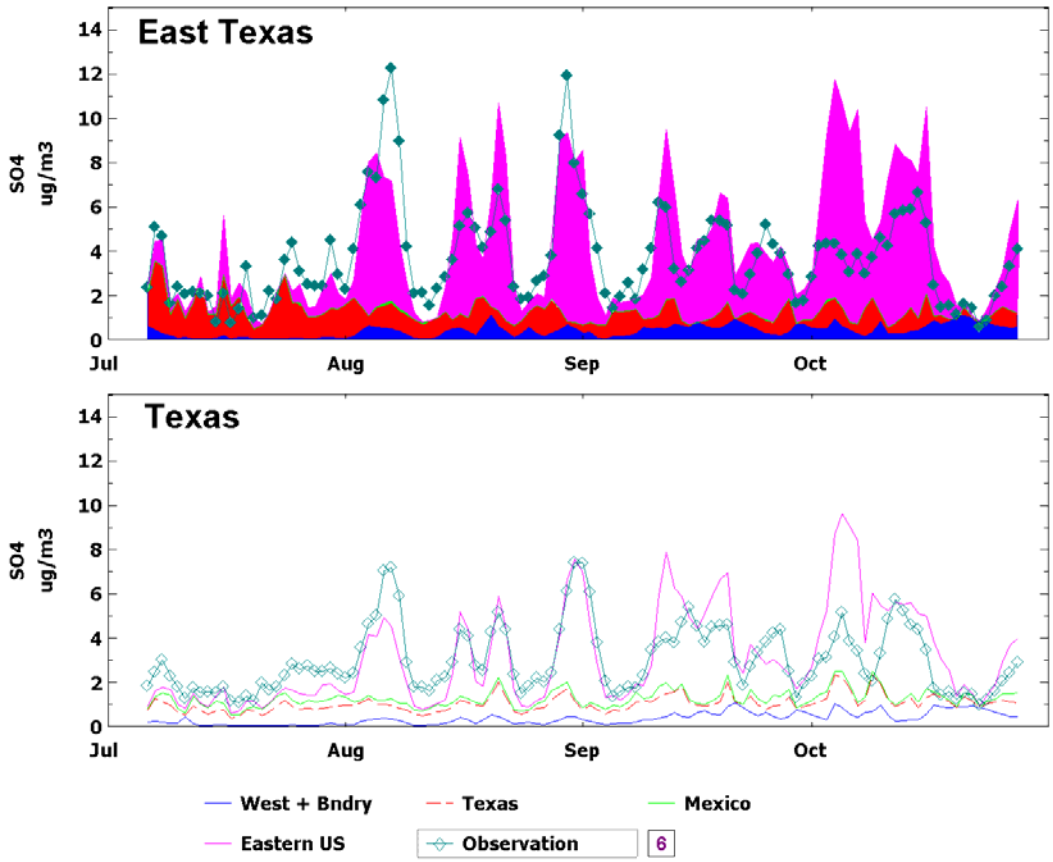

Figure 6-23. The daily source attribution average over all monitoring sites in a) West Texas, b) southern Texas, c) East Texas, and d) all of Texas. The size of the aggregation regions are defined in Figure 22. The sum of the source contribution from the four regions is approximately equal to the predicted sulfate concentrations.

The underestimation of observed sulfate throughout Texas decreased in August, and by September the REMSAD the average predicted and observed sulfate matched well overall and even overestimated the eastern Texas observed sulfate by 10–15% (Figures 6-21c and 6-23). REMSAD also captured the timing and duration of the sulfate episodes averaged over each region. The predicted sulfate in southern and eastern Texas was dominated by eastern U.S. sources. At several of the southern Texas sites the eastern U.S. source contribution was equal to or larger than the observed sulfate. This is a clear indication that the predicted eastern U.S. source attribution was overestimated at these sites. In western Texas, Mexican, Texan, and eastern U.S. sources contributed about equally to the predicted sulfate during August. All three source regions contributed to the western Texas monitoring sites during September, but sources in the eastern U.S. contributed about half of the predicted sulfate.

The results for October are presented in Table 6-8 and Figures 6-21d and 6-23. As shown, REMSAD over-predicts the measured sulfate throughout Texas. In western Texas, all four major source regions contribute to the predicted sulfate with the eastern U.S. contributing about 45%, Texas about 20%, and the western U.S. and Mexico under 15%. In south and east Texas, sources in Texas contributed 15–23% of the predicted sulfate while eastern U.S. sources contributed 65–85%. Compared to the observed sulfate concentrations the eastern U.S. source region contributed between 100–175% of the sulfate. Therefore the eastern U.S. contribution is

overestimated as far west as Eagle Pass and Fort McKavett (Table 6-8) which are only 250–350 km from Big Bend NP. Presumably, eastern U.S. contribution is overestimated in western Texas and Big Bend NP as well.

Figures 6-22 and 6-23d and Table 6-9 present the source contribution to all BRAVO sites averaged over the entire BRAVO time period. Over the four month period there is no systematic bias in the predicted sulfate compared to the observed values. Therefore the underestimation in July is compensated by the overestimation in October.

Table 6-9. The average July–October source attribution for all BRAVO monitoring sites. All units are in μg/m^3.

Region/Site	Western U.S.	Mexico	Texas	Eastern U.S.	Pred SO_4	Obs SO_4
West Texas						
Amistad	0.18	0.47	0.52	1.56	2.91	3.03
Esperanza	0.33	0.45	0.40	0.63	1.99	1.95
Fort Lancaster	0.25	0.39	0.65	1.55	3.05	3.05
Fort Stockton	0.23	0.48	0.45	0.96	2.30	2.52
Guadalupe Mtns	0.36	0.34	0.47	0.71	2.07	2.02
K-Bar	0.18	0.46	0.32	0.87	1.97	2.41
Langtry	0.20	0.50	0.53	1.51	2.95	3.47
Marathon	0.21	0.48	0.40	0.95	2.21	2.53
McDonald Obs	0.27	0.45	0.42	0.80	2.11	2.11
Monahans Sandhills	0.25	0.45	0.63	1.09	2.61	2.95
Persimmon Gap	0.22	0.48	0.40	0.98	2.24	2.71
Presidio	0.24	0.49	0.37	0.90	2.17	2.30
Sanderson	0.21	0.51	0.47	1.18	2.55	3.00
San Vicente	0.17	0.45	0.33	0.89	1.99	2.54
Average	0.23	0.46	0.45	1.04	2.37	2.62
South Texas						
Aransas	0.11	0.03	0.53	3.29	4.19	3.66
Brackettville	0.17	0.08	0.62	1.92	3.00	2.98
Eagle Pass	0.16	0.11	0.53	1.93	2.95	2.73
Falcon Dam	0.12	0.19	0.47	2.29	3.27	3.04
Laguna Atascosa	0.08	0.02	0.31	2.19	2.77	2.82
Lake Corpus Christi	0.12	0.04	0.73	2.88	4.00	3.13
Laredo	0.12	0.15	0.51	2.09	3.05	2.86
Padre Island	0.12	0.03	0.59	3.20	4.18	3.66
Pleasanton	0.12	0.06	0.94	2.32	3.64	3.17
San Bernard	0.09	0.02	0.73	3.35	4.44	3.94
Average	0.13	0.14	0.56	2.28	3.32	3.10
East Texas						
Big Thicket	0.11	0.02	0.50	4.16	5.07	4.18
Center	0.12	0.02	0.49	4.32	5.25	4.00
Everton Ranch	0.15	0.04	0.90	2.89	4.21	3.54
Hagerman	0.24	0.03	0.97	3.02	4.58	4.07
LBJ NHS	0.16	0.03	1.15	2.09	3.65	3.09

Purtis Creek	0.17	0.02	1.08	3.21	4.78	4.28
Somerville Lake	0.14	0.02	0.99	2.92	4.33	3.56
Stephenville	0.23	0.04	0.92	2.55	4.01	3.55
Stillhouse Lake	0.15	0.02	1.14	2.50	4.07	3.56
Wright Patman	0.16	0.02	0.96	4.36	5.85	4.39
Average	0.16	0.04	0.87	3.14	4.46	3.77
Other						
Fort McKavett	0.20	0.12	0.80	1.61	2.93	2.58
Lake Colorado City	0.31	0.25	0.85	1.59	3.23	2.80
Wichita Mtns	0.39	0.07	0.92	2.11	3.81	3.21
Average	0.20	0.06	0.96	2.66	4.16	3.54